RHIC Multi-Year Beam Use Request
For Run8 – Run 10

The STAR Collaboration

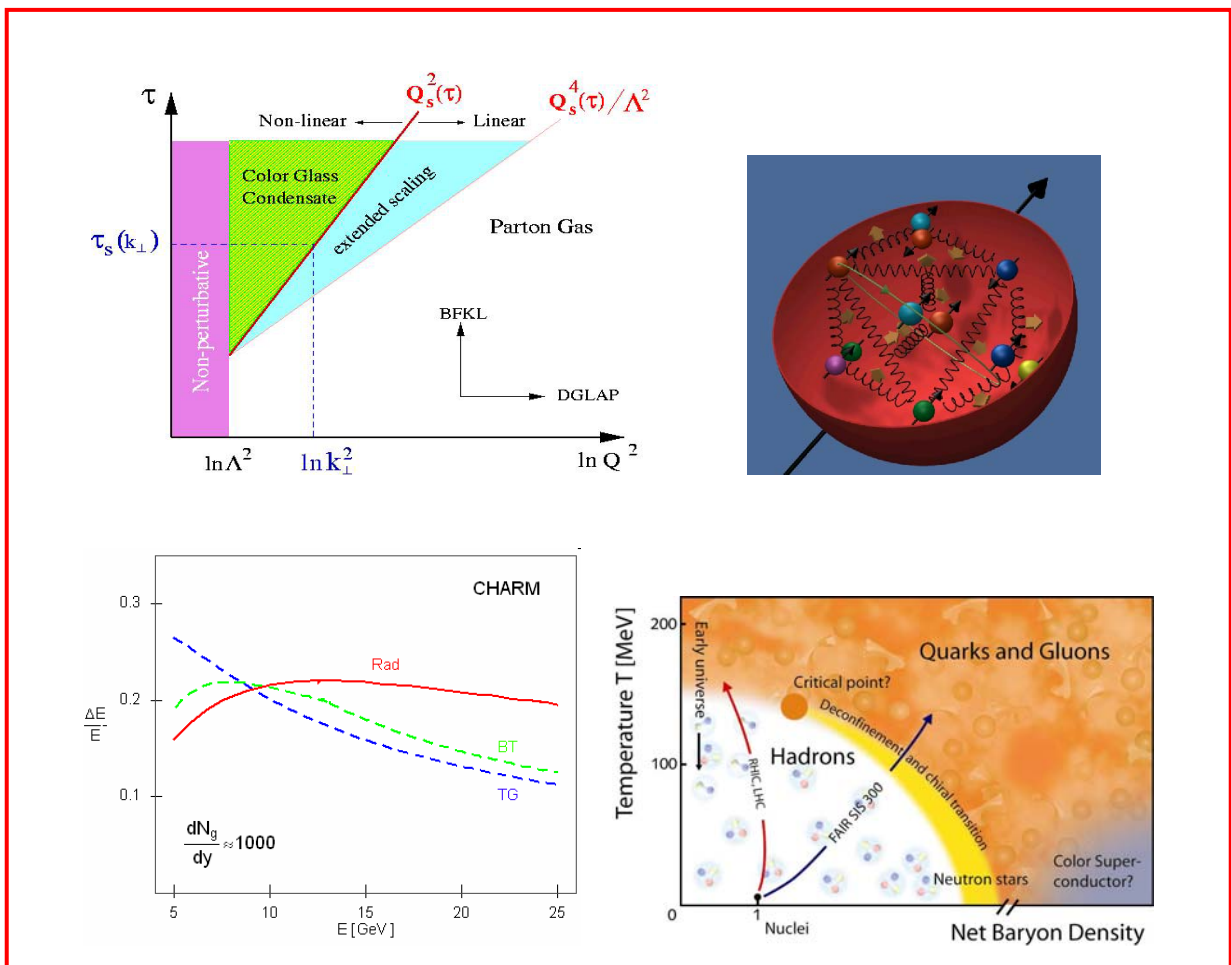## *March 18, 2007*

Table of Contents

RHIC Multi-Year Beam Use Request
For Run 8 – Run 10
The STAR Collaboration

March 18, 2007

Executive Summary

The STAR Collaboration, in order to achieve its spin and relativistic heavy ion physics goals on a timescale consistent with intense international interest and competition in these areas, as well as to utilize RHIC beams effectively taking full advantage of planned improvements in machine and detector capability as a function of time, makes the following 3 year beam use proposal:

Run	Energy	System	Goal
8	$\sqrt{s_{NN}} = 200$ GeV	d + Au	(10 + 2 weeks) 30/60 nb^{-1} sampled*
	$\sqrt{s} = 200$ GeV	$p_\rightarrow p_\rightarrow$, $p_\uparrow p_\uparrow$	(~12 + 2 weeks)
	$\sqrt{s} = 200$ GeV	$p_\uparrow p_\uparrow$	~ 3 days pp2pp
	$\sqrt{s} = 500$ GeV	pp	Commissioning**
9	$\sqrt{s_{NN}} = 200$ GeV	Au + Au	(8 + 2 weeks)
	$\sqrt{s} = 200$ GeV	$p_\rightarrow p_\rightarrow$, $p_\uparrow p_\uparrow$	(~14 + 2 weeks)
	$\sqrt{s} = 200$ GeV	$p_\rightarrow p_\rightarrow$	~ 3 days pp2pp
	$\sqrt{s} = 500$ GeV	pp	Commissioning**
10	Low $\sqrt{s_{NN}}$	Au + Au	12 + 3 weeks
	$\sqrt{s} = 500$ GeV	$P_\rightarrow p_\rightarrow$	8 + 3 weeks

* First number with slow detectors, second number with fast detectors
** Contingent on C-AD achieving efficiencies in accelerator and beam set-up

The primary physics goals of the proposed program are:

Run 8   Definitive results on the saturation scale for the gluon distribution in relativistic heavy nuclei

                      Decisive test of gluon saturation as the origin of particle suppression

at forward pseudorapidity

First significant measurement of the x dependence of gluon polarization in the proton, ΔG(x)

Qualitative advance in study of pp elastic scattering

Run 9   Qualitative advance in the study of resonances including both their hadronic and leptonic decays; extended precision in measurement of spectra and v_2 of non-photonic electrons from D, B semi-leptonic decays

Completion of initial map at √s = 200 GeV of the x dependence of gluon polarization in the proton, ΔG(x)

Run 10   Definitive search for the existence and location of the QCD Critical Point

First measurement of flavor dependence of sea quark / anti-quark polarization in the proton

The STAR Collaboration feels strongly that the proposed plan is optimal to make the most efficient use of RHIC beam time for timely progress in determining the properties of the new state of matter produced at RHIC, determining the importance at RHIC energy of gluon saturation in relativistic heavy nuclei, mapping the x dependence of the gluon polarization in the proton, ΔG(x), and performing a definitive search for the existence and (if it exists) the location of the QCD critical point.

In Run 8, the STAR proposal calls for a d+Au run of ~ 10+2 weeks duration targeted towards understanding the role of gluon saturation in the initial state wave function of entrance channel nuclei in high energy nucleus-nucleus collisions at RHIC. The remainder of the run is proposed to be polarized proton collisions for spin physics research. Building on the outstanding success in Run 6, an optimal run plan for the STAR spin physics program calls for ~30 weeks of polarized proton collision time to be divided between Run 8 and Run 9. The shortening of Run 7 makes it impossible to achieve this goal fully, but the STAR proposal for Runs 8 and 9 comes very close. The highest priority for the use of this time will be longitudinal spin running at $\sqrt{s} = 200$ GeV, allowing a significant map of the *x*-dependence of the gluon polarization, within the approximate range 0.03 < *x* < 0.3. Smaller values of *x* will subsequently be probed in 500 GeV running. Modest amounts of running time to attack priority goals of the transverse spin program using the extended capability provided by the STAR Forward Meson Spectrometer are also anticipated. During Run 8, STAR strongly supports continued polarization development of proton beams in the AGS, in parallel with RHIC stores. Contingent on C-AD achieving efficiencies in accelerator and beam set-up, commissioning time dedicated to preparing for a future √s = 500 GeV polarized proton run is proposed.

In Run 9, a primary goal will be utilization of the newly complete DAQ1000 upgrade and and partially complete TOF upgrade to extend STAR's scientific reach significantly for measurement of hadronic and leptonic decays of resonances. The "near-zero-mass" configuration of the interior elements of the STAR detector during this period will also result in a significant extension of previous measurements of the spectra and v_2 of electrons from semi-leptonic decays of D and B mesons. Data taken with polarized protons during Run 9 should substantially complete STAR's initial map at $\sqrt{s} = 200$ GeV of the spin-dependent gluon distribution as a function of momentum fraction, $\Delta G(x)$. Contingent on C-AD achieving efficiencies in accelerator and beam set-up, commissioning time dedicated to preparing for a future $\sqrt{s} = 500$ GeV polarized proton run is proposed in Run 9 as well.

The primary heavy ion physics goals for Run 10 will be to establish the possible existence of a critical point in the phase diagram for QCD matter by carrying out a comprehensive search for critical fluctuations as a function of $\sqrt{s_{NN}}$ in Au+Au collisions. First measurement of the flavor dependence of the sea quark/anti-quark polarization in the proton will also be carried out by studying parity violating $W^{\pm}$ decays in polarized proton collisions at $\sqrt{s} = 500$ GeV.

1. Beam Use Proposal for Run 8

1.1 Previous d+Au physics results and scientific motivation of d+Au measurements proposed for Run 8

The low-x structure of heavy nuclei is a fundamental question of great interest, both in its own right and because it determines the initial conditions in relativistic heavy ion collisions. For protons, data from HERA show that the low-x region is dominated by gluons and that gluon splitting causes the gluon density to increase dramatically as x is decreased. At a sufficiently small value of x, yet to be determined by experiment, the splitting is expected to become balanced by recombination as the gluons overlap in the transverse plane, resulting in gluon saturation. Indeed, some theorists have argued that the HERA results already point to an onset of gluon saturation effects in the proton in the region $x <\sim 0.01$. In contrast, others have argued that conventional DGLAP evolution, which should only be appropriate in the dilute regime, applies over the entire HERA kinematic domain. Overall, the picture is clouded by the lack of a well-defined "unsaturated" baseline system to which the HERA data can be compared.

The gluon density in a heavy nucleus is larger than that in the proton by a factor of $\sim A^{1/3}$. This makes heavy nuclei particularly attractive laboratories to look for saturation effects for two reasons. The increased gluon density implies saturation effects should become apparent at higher values of x in nuclei than in the nucleon. Meanwhile, the measured gluon density in the nucleon provides a well-defined reference for comparison.
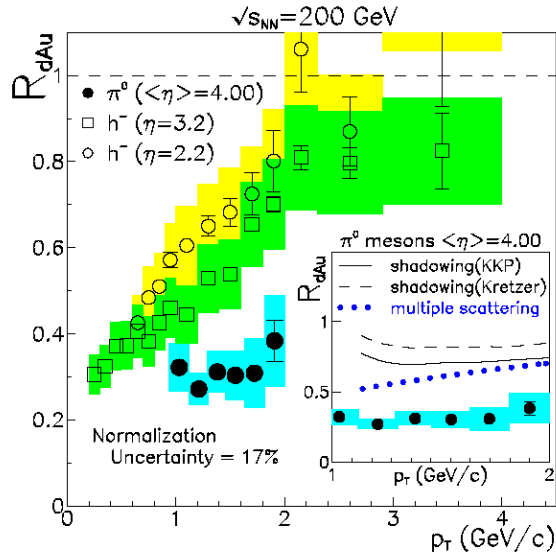

Figure 1: Nuclear modification factor R_{dAu} vs. p_T for identified π^0 at $\eta=4$ from STAR [1], compared to previous BRAHMS results for unidentified h^- at $\eta=2.2$ and 3.2 [2]. The inset shows the STAR results compared to several theoretical predictions. See [1] for details.

Measurements of inclusive particle production in d+Au collisions at RHIC have established that the yield of produced particles systematically decreases as their rapidity increases. For example, Fig. 1 shows recent results for the nuclear modification factor R_{dAu} for identified π^0 at $\eta=4$ from STAR [1], compared to previous results for unidentified h^- from BRAHMS [2]. The inset shows a comparison of the STAR results to several theoretical predictions, all of which predict much less suppression than is observed. The BRAHMS results at forward rapidity have been described by calculations [3] based on the Color Glass Condensate (CGC) model that treats the Au nucleus as a saturated gluon field. As shown in Fig. 2, calculations within the CGC model [4] also provide a very good description of the p_T dependence of the π^0 cross section measured by STAR, although they overpredict the observed π^0 yield at $\eta=4$ by a factor of ~2 when they are scaled to match the BRAHMS results at $\eta=3.2$.
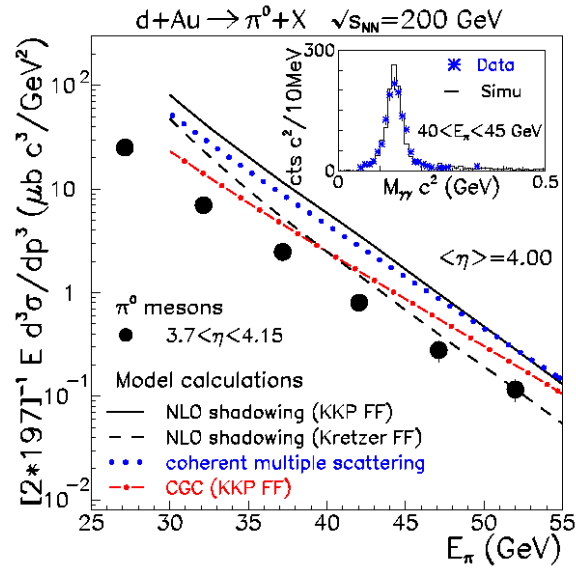

Figure 2: Inclusive π^0 cross section per binary collision for d+Au collisions at $\eta=4$. The curves are model calculations, and are described in detail in [1]. The inset shows a comparison between the uncorrected di-photon invariant mass spectra from data and from Monte Carlo simulations.

To further elucidate the dynamics underlying particle production in d+Au collisions at forward rapidity, STAR also performed exploratory measurements of forward-midrapidity di-hadron coincidences during Run 3 [1]. Many models that predict the yield of particles should be suppressed in d+Au collisions, including those that attribute the suppression to conventional leading-twist shadowing or initial-state energy loss, nonetheless expect that back-to-back correlations, characteristic of di-jets, should remain similar. In contrast, in the saturation picture, forward particles arise from energetic quarks in the deuteron that undergo multiple interactions in the dense gluon field of the Au nucleus, leading to an apparent "mono-jet" mechanism [5].

Figure 3 shows the probability of finding a leading charged particle with $p_T > 0.5$ GeV/c at midrapidity in coincidence with an identified π^0 at $\eta=4$. Results are shown for p+p and

d+Au collisions, and for two different π^0 energy ranges. (Note that $p_T = E_\pi / \cosh \eta$.) A PYTHIA simulation predicts most of the features of the p+p data [1]. HIJING simulations with nuclear shadowing predict the d+Au correlations should be qualitatively similar to those in p+p. HIJING provides a reasonable description of the d+Au data in the $30 < E_\pi < 55$ GeV bin, including both the strength of the coincidence peak and the magnitude of the combinatoric background. In contrast, the low E_π data are not consistent with the HIJING expectations. Very recently PHENIX has published results of a similar d+Au forward-midrapidity correlation study [6]. However, the PHENIX measurements are sensitive to significantly larger x_g values than are sampled in the STAR study, so it is not clear that one should expect similar behavior.
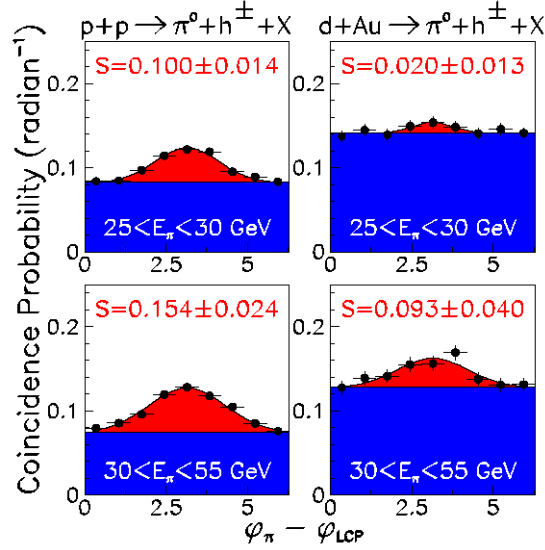

Figure 3: Coincidence probability vs. $\Delta\varphi$ between a forward π^0 at $\eta=4$ and a leading charged particle with $p_T > 0.5$ GeV/c and $|\eta| < 0.75$. The curves show fits to a Gaussian centered at $\Delta\varphi = \pi$ plus a constant background. The term "S" indicates the area of the back-to-back peak.

The existing d+Au results suggest that forward particle production at RHIC may be sensitive to the onset of gluon saturation. However, many alternate explanations of the observed effects have been offered, including limiting fragmentation, parton recombination, initial-state energy loss, and factorization breaking. In fact, there is even controversy regarding the kinematic range that is explored by the existing RHIC d+Au results. Perturbative QCD calculations predict that the $\langle x_g \rangle$ sampled by the BRAHMS measurement is ~0.02 [7], whereas CGC calculations imply the $\langle x_g \rangle \sim 0.001$ [4]. Thus, evidence for gluon saturation at RHIC energies is not yet conclusive.

Unambiguous determination of the gluon density in a heavy nucleus requires going beyond inclusive particle production to explore particle correlations in order to elucidate the dynamics that underlie the observed suppression of the inclusive yields. Perturbative

QCD is known to describe inclusive hadron yields at forward rapidity in p+p collisions at RHIC, especially for $p_T >\sim$ 2 GeV/c (e.g., see Fig. 4). In pQCD, triggering on particle production in the forward direction implies that the quarks from the deuteron beam are the predominant probes of the gluons in the Au nucleus. The gluon density in the Au nucleus is probed at the lowest Bjorken x values when pairs of jets, or their hadronic surrogates, are both observed at large rapidity.

It is important to quantify whether the gluon density in the Au nucleus saturates at RHIC energies. Knowledge of the quark and gluon distributions in the gold nucleus is essential for understanding the initial state of a Au+Au collision, and how that state evolves on apparently very short time scales into a strongly interacting quark gluon plasma. We know that most of the mass of protons and neutrons arises from the very strong color fields carried by the gluons that bind the nearly massless up and down quarks. But, we
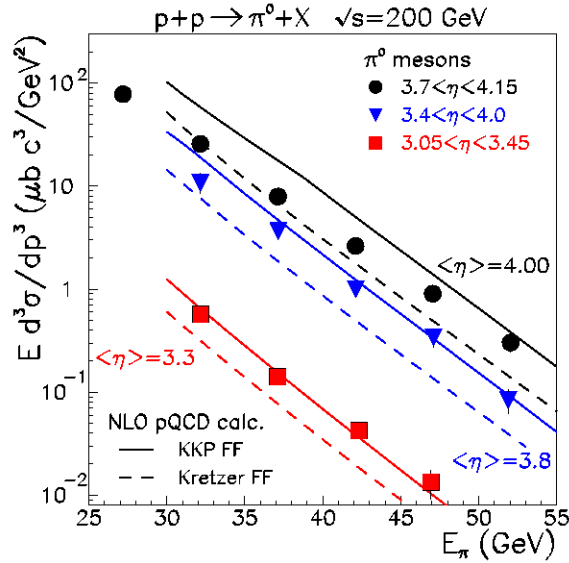
Figure 4: Inclusive π^0 cross section in p+p collisions vs. E_π, compared to NLO pQCD calculations that assume two different fragmentation functions. See [1] for details.

have essentially no knowledge about the gluon density in a heavy nucleus. It is expected that at the LHC a saturated gluon density will be manifest in p+p collisions in forward particle production and in ion collisions over the entire rapidity range, so it is timely to quantify the role of gluon saturation at RHIC prior to the start of operations of the LHC.

The low-x gluon density in the Au nucleus can be measured in d+Au collisions at RHIC through correlated particle measurements. In pQCD, *inclusive* forward particle production in high energy hadronic collisions probes the gluon density over a broad range of Bjorken x values [7]. The x value can be much better constrained through measurement of back-to-back pairs of particles. When an away-side hadron is detected in

coincidence with a leading hadron or jet at forward rapidity, the pseudorapidity of the recoil jet or its hadronic surrogate reflects the x value probed. This is illustrated for p+p collisions in Fig. 5. The lowest x values are reached when both particles are detected in the forward direction [8].

The STAR Forward Meson Spectrometer (FMS) (Fig. 6) has been assembled to enable measurement of the gluon densities in the Au nucleus down to x values where saturation is expected to become apparent. It is ready for commissioning when beam turns on for Run 7. The FMS spans the pseudorapidity interval $2.5 < \eta < 4.0$. This will give STAR nearly hermetic electromagnetic calorimetry over the range $-1 < \eta < 4$. This broad coverage will enable the mapping of the nuclear gluon density down to $x \sim 0.001$
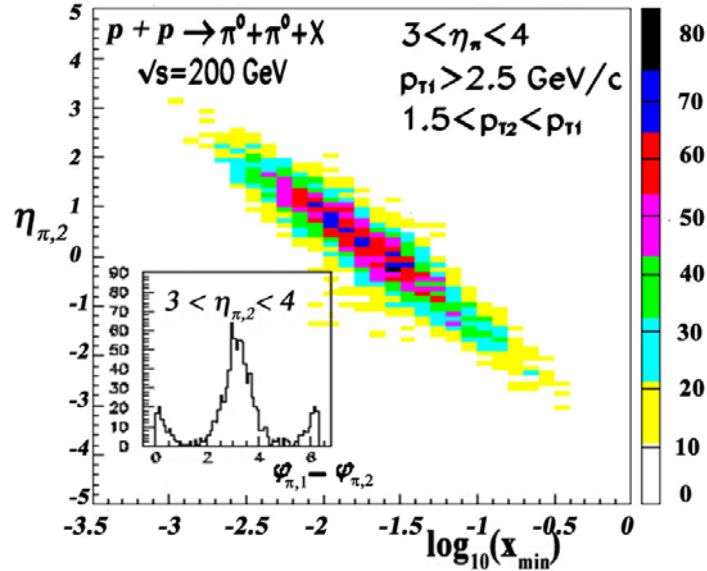
Figure 5: PYTHIA predictions for the correlation between η_2 and x_{min} for $p+p \rightarrow \pi^0 + \pi^0 + X$, where the first π^0 has $3 < \eta_1 < 4$ and $p_{T,1} > 2.5$ GeV/c, and the second π^0 obeys 1.5 GeV/c $< p_{T,2} < p_{T,1}$. The inset shows the corresponding $\Delta\varphi$ distribution.

utilizing particles with sufficiently high p_T that the corresponding p+p collisions are well described by pQCD.

The FMS will dramatically increase STAR's forward physics capabilities. The FMS covers a solid angle nearly three times that of the FPD++, which it has replaced (and 16 times the area of the west FPD, which was replaced by the FPD++ prior to Run 6). At least as important, only a small fraction of the Pb-glass cells in the FPD++ participated in the trigger decisions. In contrast, all of the Pb-glass cells in the FMS will feed the trigger logic. This will provide nearly an order of magnitude increase in the trigger coverage.
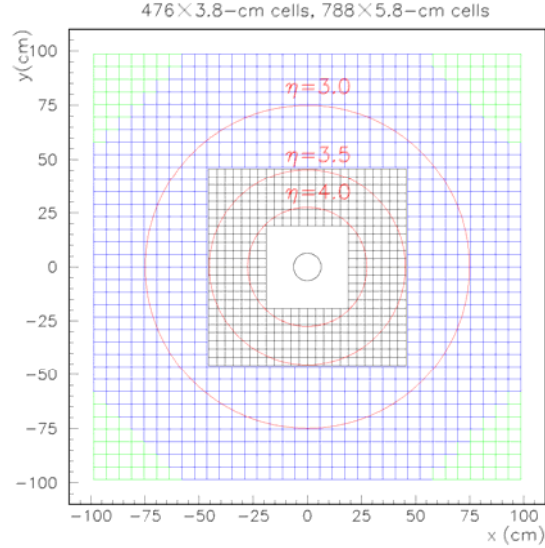
Figure 6: Front view of the STAR Forward Meson Spectrometer (FMS). The FMS consists of 1264 Pb-glass cells and cover the pseudorapidity region $2.5 < \eta < 4$. The FMS greatly expands STAR's acceptance for mesons decaying into photons and for meson coincidences in a kinematic region where particle production is dominated by contributions that are sensitive to low-x gluons in the Au nucleus.
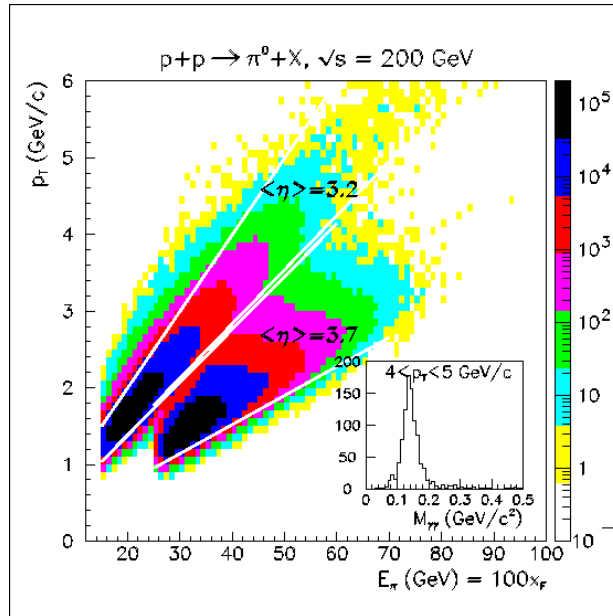
Figure 7: Kinematic coverage of the forward π^0 data from the 200 GeV p+p transverse spin period of Run 6. The η=3.7 band represents events that were detected by the east FPD. The η=3.2 band represents events that fell within the triggered fraction of the FPD++. The FMS will span this entire area, including the gap between the two regions. It will also extend the coverage to smaller η, providing even higher p_T reach at any given x_F. The inset shows the invariant mass spectrum for the 2-photon events with $4 < p_T < 5$ GeV/c, demonstrating the clean π^0 reconstruction.

Preliminary data from Run 6, as shown in Fig. 7, provide an indication of the capabilities that can be expected from the FMS.

1.2 d+Au beam use request for Run 8

The STAR Collaboration proposes 10+2 weeks of d+Au running at $\sqrt{s_{NN}}$ = 200 GeV to provide definitive results on the gluon saturation scale in relativistic Au nuclei, and to determine if gluon saturation accounts for the suppression of inclusive particles observed at forward pseudorapidity at RHIC. The requested data set will also provide reference data essential for comparison with $\sqrt{s_{NN}}$ = 200 GeV Au+Au data from Run 7.

It is important to determine if gluon saturation is the correct explanation for the existing RHIC data. The saturation scale represents a fundamental property of hadrons and nuclei. Indeed, one saturation theory that has been quite successful, the Color Glass Condensate, predicts that there exists a universal wave function for hadronic matter at sufficiently high energy or small x. Even if gluon saturation does not prove to be the correct explanation, it is nonetheless crucial to determine the gluon density at small x in the Au nucleus if one hopes to understand the initial state in Au+Au collisions at RHIC and its rapid evolution from a highly non-equilibrated system to a thermalized one.

RHIC is uniquely situated to explore this phenomenon. We know that the gluon density ultimately must saturate, but a fundamental question is: *When does it occur?* For example, the gluon density at the saturation momentum controls such basic properties of heavy-ion collisions as the multiplicity. To observe the onset of saturation, it's essential to be able to turn it on and off. This will likely be possible at RHIC, making it the ideal laboratory to explore the underlying mechanism for saturation. In contrast, particle production in heavy-ion collisions at the LHC may occur deep within the saturation regime over most of the accessible kinematic region. If that proves to be the case, then (a) it will be very difficult to turn saturation effects off at the LHC, and (b) it will be essential to quantify the saturation effects independently in order to distinguish between initial-state saturation effects vs. final-state plasma effects in Pb+Pb collisions at the LHC.

The *RHIC Collider Projections (FY2007-2008)* document indicates that we can expect RHIC to deliver ~120 nb^{-1} of d+Au collisions at $\sqrt{s_{NN}}$ = 200 GeV during a 10-week physics run. (This is the average of the projected minimum and maximum performance estimates.) STAR proposes to utilize the d+Au collisions as follows:

- Fast-detector data (e.g., FMS, BEMC, EEMC, BBC, etc.) will be recorded with essentially 100% livetime for events that include an intermediate- or high-p_T π^0 in the FMS. Previous analyses of FPD and FPD++ data indicate that a very high fraction of these events will be usable.

- Slow-detector data (e.g., events that include read-out of the TPC, FTPC, etc.) will be recorded at 50 Hz, leading to 50% livetime. The approximate division of this bandwidth will be:
  - Minbias: 30 Hz
  - BEMC and EEMC high-tower triggers: 10 Hz
  - FMS triggers: 10 Hz

Detailed simulations, such as those in Fig. 8, have established that the fast-detector events will permit STAR to map out the gluon density in the gold nucleus over the range $0.001 \leq x \leq 0.1$. If we assume $R_{dAu} \sim 0.5$ for the trigger π^0 in Fig. 8 obtained by extrapolating the results in Fig. 1 to the trigger kinematics, and also assume that $2 \rightarrow 2$ partonic scattering dominates particle production as would be expected in pQCD, the requested luminosity would yield approximately $10,000 \pm 170$ events in the coincidence peak. The region $1 < \eta_{\pi,2} < 4$ in Fig. 8 corresponds approximately to the region $0.001 <\sim x <\sim 0.01$ where we might hope to find evidence for gluon saturation. This sample will be sufficient to allow examination of the x dependence of the gluon density in 3~4 centrality bins, even if the recorded statistics end up much reduced because gluon saturation effects are found. It will also facilitate important cross-checks of the conclusions. For example, the kinematic coverage will be sufficiently broad so that the same x_g will be sampled with trigger π^0 over a range of x_F values. The latter closely approximate the x of the scattered quark from the deuteron beam, so this study will provide an independent means to distinguish between gluon saturation and incident quark energy loss. Data will be taken concurrently in the region $-1 < \eta_{\pi,2} < 1$, corresponding to $0.01 <\sim x <\sim 0.1$. These data will be compared to existing nuclear deep-inelastic lepton scattering measurements to provide an important universality check.
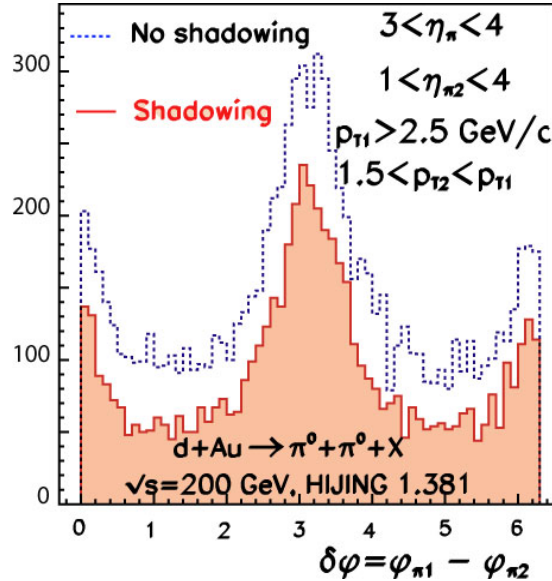

Figure 8: HIJING predictions for the $\Delta\varphi$ distribution in d+Au collisions, with and without shadowing. HIJING includes leading-twist shadowing, which leads to a reduction in the coincident peak yield, without a significant change in its structure.

As noted above, the ability to compare results from d+Au collisions to reference results from p+p collisions is very important. The analyses of the Run 8 d+Au data will use p+p data also taken from Run 8 to provide reference data over a broad kinematic range.

The proposed 30 Hz of slow-detector minbias data will provide 60 M events. These will be used to obtain high statistics comparison data for Au+Au measurements made during Run 7. The high-tower triggered data will provide a dramatic improvement in STAR measurements of non-photonic electrons over those from previous d+Au running. Finally, the 10 Hz of slow-detector data triggered with the FMS will provide measurements of correlations between triggered π^0 and coincident charged particles to complement the π^0 - π^0 correlations that will be obtained from the fast-detector data. This will facilitate important studies of the near-side jet structure, utilizing the pseudorapidity coverage of the FTPC. These data will also open the possibility to measure forward J/ψ by combining the complementary features of the FMS and FTPC.

2. Polarized proton results, progress and proposed running for Run 8

2.1 Report on polarized proton data taking in Run 6

The scientific priority for the STAR program in Run 6 was to obtain a deeper understanding of the spin structure and dynamics of the proton by studying how the intrinsic spin of the proton is distributed among its underlying constituents (quarks, anti-quarks, and gluons). The data acquisition targets for Run 6 are shown in Table 1. As shown in the table, the goals for Run 6 were all substantially met as reported last fall.

Table I: Data acquisition goals for Run 6

Energy $\sqrt{s_{NN}}$ (GeV)	Trigger	System	Acquired	Goal
200 (longitudinal)	Rare (BEMC /EEMC Triggered)	p + p	8.5 pb^{-1}, P ~ 60% FOM ~ 830 nb^{-1}	10 pb^{-1}, P ~ 50% FOM ~ 625 nb^{-1}
200 (transverse)	Rare (Di-Jet)	p + p	3.34 pb^{-1} sampled, P ~ 60%	~3 pb^{-1} sampled* P ~ 50%
200	L2 J/Ψ	p + p	3.17 M events	3 M events
62.4	Minimum Bias	p + p	16.2 M events	15 M events

* This goal decreased from 5 pb^{-1} due to a very good L2 Di-jet Trigger

STAR sampled a total of approximately 8.5 pb^{-1} with longitudinal beam polarization and approximately 3.4 pb^{-1} (slow detector) / 6.8pb^{-1} (fast detectors) with transverse beam polarization at $\sqrt{s}$ = 200 GeV. In addition, at the end of Run 6, STAR collected a total of 0.1 pb^{-1} at $\sqrt{s}$ = 62 GeV using transversely polarized beams. The longitudinal data sample

was split between an initial sample of 2.1 pb^{-1} during the beginning of Run 6 and 6.4 pb^{-1} at the end of the 200 GeV data taking period. These two samples were separated by data taking with transversely polarized beams. Beginning with the start of the transverse running period at $\sqrt{s} = 200$ GeV, the average beam polarization in both RHIC beams was ~60%.

During Run 6, significant improvements in RHIC's capability as a polarized proton-proton collider as well as in STAR detector acceptance and trigger capability resulted in a dramatic change in the quality, magnitude, and richness of the spin data acquired. The simultaneous improvements in integrated luminosity and polarization in 2006 yielded at least a factor of 4 gain in the figure of merit LP^4 compared to 2005 for the measurement of any double spin asymmetry while allowing for significant running time with longitudinal polarization.

The result of these advances in the quality of the beam delivered and STAR's ability to mine the collisions was a Run 6 data set that far surpassed all previous polarized proton runs in terms of physics content. The combination of extended calorimetric coverage, reduction of the background trigger rate, and more intelligent triggering decisions increased the size the recorded di-jet sample by almost an order-of-magnitude per unit integrated luminosity compared to 2005. From these data, quantitative estimates of the magnitudes of the gluon and quark Sivers functions in several kinematic regions are being extracted to compare to existing results from semi-inclusive DIS [9,10]. Data taken with the FPD are allowing STAR to map out the x_F and p_T dependences of the large neutral pion spin asymmetries observed earlier in STAR at high rapidity, and to search for jets and direct photons in this regime. The longitudinally polarized runs have extended the existing STAR results on A_{LL} for inclusive jets and neutral pions to higher p_T, and, due to improvements in triggering and acceptance, they have provided the first substantial sample of di-jets. The Run 6 data set should also yield the first useful sample of photon-jet coincidences which will be crucial to the development of algorithms for identifying direct photons in the EMC's in order to reconstruct the photon-jet events to probe the x dependence of the gluon helicity preference in the proton. Further progress on the Run 6 physics analysis will be discussed in the next section.

2.2 Recent spin physics results and proposed measurements for Run 8

Many preliminary results [11-18] based on 2005 pp data and two on 2006 data were released at SPIN 2006. We summarize these below.

2.2.1 STAR transverse spin program - recent results

The study of transverse spin effects, both theoretically and experimentally, has received a lot of attention in recent years. The ultimate goal of this effort is to extract transversity distribution functions and determine possible orbital angular momentum contributions of quarks, anti-quarks and gluons to the proton spin [18].

The first measurement of a transverse single-spin asymmetry, A_N, for forward neutral pion production at $3.3 < \eta < 4.1$ by the STAR collaboration [19] was found to increase with x_F similar in magnitude to the measurement of A_N performed by the E704 experiment at $\sqrt{s}$ =20 GeV [20]. The STAR collaboration has performed cross-section measurements for forward neutral pion production at $<\eta>$=3.3, 3.8 and 4.0, which are found to be in good agreement with next-to-leading order (NLO) perturbative QCD calculations [21]. This provides an important basis for the interpretation of the sizable measured asymmetries at forward rapidity. Several models beyond a conventional collinear perturbative QCD approach are able to account for the measured asymmetries. These models are based on three main correlation concepts: A correlation of the parton intrinsic transverse momentum k_T and the proton spin in the initial state (Sivers effect) [22], a correlation between the quark spin and the hadron k_T in the final state (Collins effect) [23] and a higher twist correlation in the initial and final state [24, 25]. The STAR collaboration performed an upgrade of the Forward Pion Detector (FPD) for Run 6 as a prototype for the Forward Meson Spectrometer (FMS). The main goal is to disentangle different mechanisms responsible for the observed large transverse single-spin asymmetries in the forward direction. New results for forward neutral pion production at higher precision are shown in Figure 9. [13]. These results are in good agreement with previous results. The measured asymmetry A_N is found to be consistent with zero at negative x_F and grows from 0 at $x \sim 0.2$-0.3 up to 0.1 at $x_F \sim 0.6$. The figure also shows the results of two calculations at different $<\eta>$ values [26,27]. The measured asymmetries
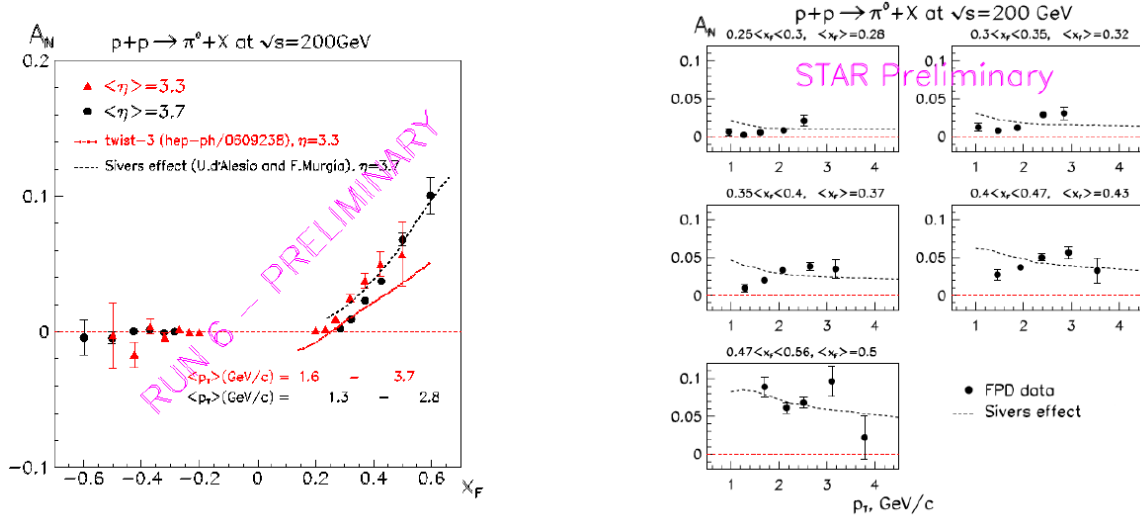
Figure 9: (Left) A_N as a function of x_F for p+p $\rightarrow \pi^0$+X from Run 6. The error bars represent statistical errors only. Systematic uncertainties are smaller than statistical uncertainties. The dotted line represents the result of a twist-3 calculation [26]; the dashed line is the result of a calculation based on the Sivers effect [27]. (Right) A_N as a function of p_T for p+p $\rightarrow \pi^0$+X from Run 6 in bins of x_F in comparison to a calculation based on the Sivers effect [27].

are precise enough to allow for a quantitative comparison with theory predictions. The extended kinematic region in x_F and p_T and the increase in the available data sample from Run 6 allow a mapping of A_N in x_F and p_T for the first time. Figure 9 (right) shows A_N as a function of p_T in fine bins of x_F. The current measured results for A_N do not support a decreasing behavior of A_N with p_T in all x_F bins as expected by various theoretical models.

A possible manifestation of orbital angular momentum effects could be realized through a non-zero Sivers type correlation of the parton intrinsic transverse momentum k_T and the proton spin in the initial state. The HERMES collaboration recently reported a non-zero Sivers function in semi-inclusive DIS for π^+ production [28]. The Sivers function for π^- production has been found to be consistent with zero. This led to the interpretation that the Sivers functions are opposite in sign and different in magnitude for u quarks compared to d quarks. The study of Sivers type correlations in polarized proton-proton collisions has been considered in ref. [29]. The theoretical expectation is that the Sivers effect
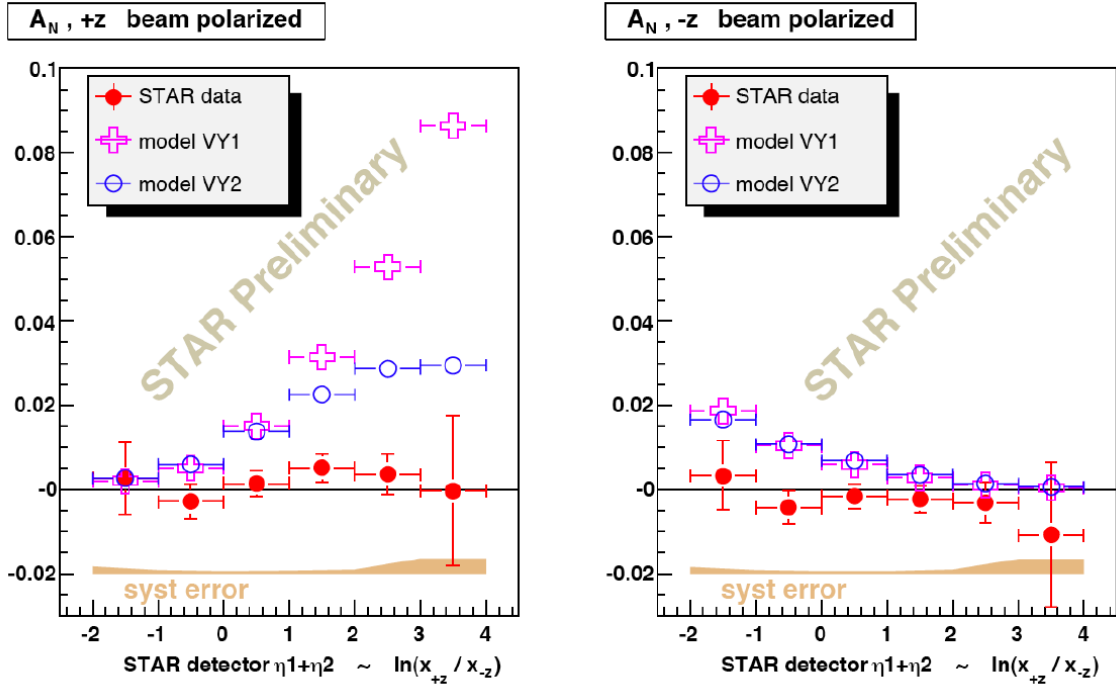
Figure 10: Transverse single-spin asymmetries for A_N^{+z} (left) and A_N^{-z} (right) as a function of $\eta_1+\eta_2$ for di-jet production at $\sqrt{s} = 200$ GeV from Run 6 in comparison to theoretical calculations [10,30].}

would be reflected in a spin-dependent side-ways boost observed as a corresponding spin-dependent asymmetry in the back-to-back di-jet opening angle. A measurement of the correlation between the spin direction and di-jet bi-sector direction was performed to

search for this effect. A dedicated Level 2 di-jet trigger, utilizing the STAR Barrel and Endcap Electromagnetic Calorimeters (BEMC and EEMC), was implemented during Run 6 to provide a sufficient sample of di-jet events for the study.

Figure 10 shows the measured transverse single-spin asymmetry, A_N, for di-jet production as function of $\eta_1+\eta_2$ [11]. The region of large $\eta_1+\eta_2$ values emphasizes quark (gluon) Sivers effects for +z (–z). In both cases, the measured transverse single-spin asymmetries are found to be consistent with zero. The measured results are compared to predictions based on u and d quark Sivers functions extracted from measured HERMES semi-inclusive DIS data, which assume a zero gluon-type Sivers function [10,30]. The calculations were carried out using only gauge-link factors for initial-state interactions, as expected for Drell-Yan production. Recent theoretical work has added modifications required for di-jet production which take into account final-state effects [31].

2.2.2 STAR longitudinal spin program - recent results

The longitudinal STAR spin physics program profits enormously from the unique capabilities of the STAR experiment for large acceptance jet production, identified hadron production and photon production [32]. The measurement of the gluon polarization through inclusive measurements such as jet production and π^0 production has so far been the prime focus of the physics analysis program of the Run 3/4 and Run 5 data samples. The sensitivity of these inclusive measurements to the underlying gluon polarization in high-energy polarized proton-proton collisions has been discussed in detail in [33]. Inclusive hadron production and jet production are strongly affected by the relative contributions from quark-quark, quark-gluon and gluon-gluon subprocesses. The low p_T region is dominated by gluon-gluon scattering, while at high p_T the quark-gluon contribution starts to become important. As a result, the sign of A_{LL} in this high p_T region indicates the sign of the gluon polarization. The fact that the inclusive photon channel is dominated by quark-gluon scattering results in a strong sensitivity to the underlying gluon polarization, despite the small production cross-section. Throughout the following discussion, four gluon polarization scenarios have been used as input to NLO perturbative QCD calculations of A_{LL}. The GRSV standard case refers to the best global analysis fit to polarized DIS data [34]. The case for a vanishing gluon polarization (GRSV-ZERO) and the case of a maximally positive (GRSV-MAX) or negative (GRSV-MIN) gluon polarization have been also considered.

The first longitudinal double-spin asymmetry measurement for inclusive jet production and the associated inclusive jet cross-section measurement at mid-rapidity has recently been published [35]. The measured asymmetries are consistent with NLO perturbative QCD calculations based on DIS polarized lepton-nucleon data, and disfavor a large positive value of the gluon polarization in the proton. In addition, the STAR collaboration has recently released a preliminary result on the inclusive neutral pion production cross-section at mid-rapidity [36]. The (unpolarized) cross-section measurements of inclusive

jet and neutral pion production support the asymmetry measurements at RHIC by validating the applicability of perturbative QCD.

The following measurements of A_{LL} from Run 5 at $\sqrt{s} = 200\,\text{GeV}$ [12,14,15,16] for identified hadron production and inclusive jet production are based on an average beam polarization of approximately 50% and a data sample of approximately 3 pb^{-1}. The overall normalization uncertainty due to conservative error estimates on the preliminary polarization values amounts to ~40%. All A_{LL} analyses presented below make use of the STAR BEMC and EEMC system at the trigger and reconstruction level. A high-tower (HT1 / HT2) trigger is based on an energy threshold above 2.8 (3.8) GeV for a single tower ($\Delta\eta$ x $\Delta\phi$ = 0.05 x 0.05) whereas a jet-patch (JP1 / JP2) trigger is based on an energy threshold above 4.5 (6.5) GeV for a group of towers over a region in η and ϕ of $\Delta\eta$ x $\Delta\phi$ = 1.0 x 1.0. Both triggers are taken in coincidence with a minimum-bias condition using the STAR Beam-Beam Counter.
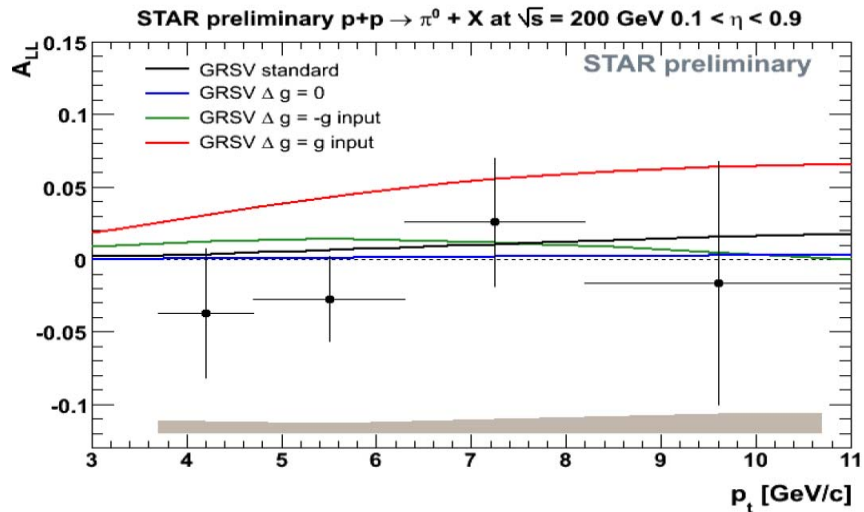

Figure 11: Longitudinal double-spin asymmetry A_{LL} for neutral pion production at $\sqrt{s} = 200$ GeV as a function of p_T (0.1 < η < 0.9) for Run 5 in comparison to several gluon polarization scenarios.

Figure 11 shows the measured longitudinal double-spin asymmetry A_{LL} for neutral pion production as a function of p_T together with different gluon polarization scenarios as described above. The error bars include statistical uncertainties only. The systematic error band includes contributions from the neutral pion yield extraction and background subtraction, remaining background, possible non-longitudinal spin contributions and the relative luminosity uncertainty. This analysis is based on a fraction of the Run 5 data sample for a restricted pseudo-rapidity region. Data from Run 6 will include the full acceptance of the STAR BEMC. The data tend to disfavor a large positive gluon polarization scenario.

In addition to the first neutral pion analysis of A_{LL} at mid-rapidity, the STAR collaboration has recently presented the first preliminary result of neutral pion production using the STAR EEMC in the pseudo-rapidity acceptance region of $1.086 < \eta < 2.0$ from Run 5 [18]. The data are consistent with zero over the p_T range of $3 < p_T < 7$ GeV/c, albeit with large statistical uncertainties. The systematic uncertainties are comparable to the statistical uncertainties and dominated by beam induced background. These background contributions were observed to be suppressed by a factor 20 during Run 6 relative to those in Run 5 profiting from the installation of shielding to reduce beam induced background between the runs. This EEMC based analysis provides an important baseline measurement for future prompt photon measurements in the STAR EEMC acceptance region.
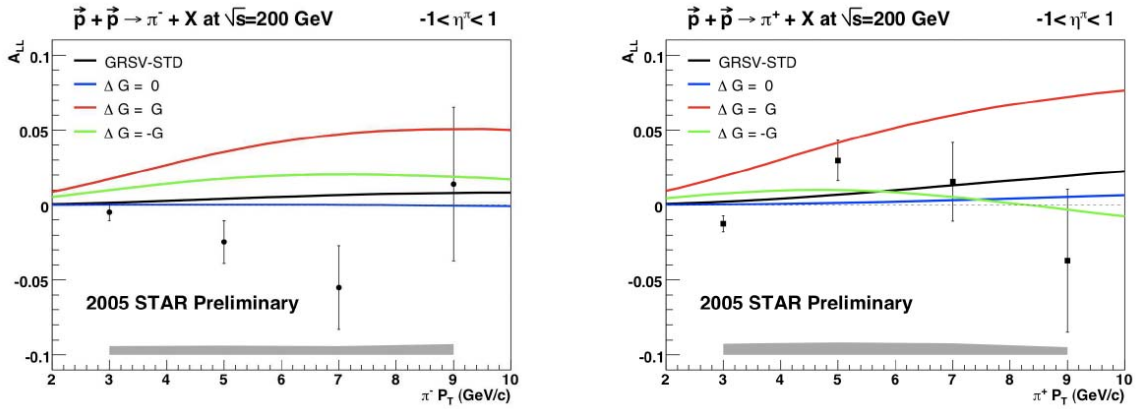

Figure 12: Longitudinal double-spin asymmetry A_{LL} for charged pion production at $\sqrt{s} = 200$ GeV as a function of p_T (-1 < η < 1) for Run 5 in comparison to several gluon polarization scenarios.}

The STAR collaboration has also presented the first measurement of the longitudinal double-spin asymmetry A_{LL} for inclusive charged pion production from Run 5. The asymmetries are calculated over the transverse momentum region $2 < p_T < 10$ GeV/c and compared to several gluon polarization scenarios as described earlier. This analysis is unique in that the difference $A_{LL}(\pi^-)$ - $A_{LL}(\pi^+)$ tracks the sign of the gluon polarization, due to the opposite signs of the polarized distribution functions for up and down quarks. The STAR TPC offers robust reconstruction and identification of charged pions over the transverse momentum range $2 < p_T < 10$ GeV/c. Particle identification in the TPC is accomplished using measurements of ionization energy loss of TPC hits. Figure 12 shows preliminary results during Run 5 for charged pion production. The measured asymmetries are compared to theoretical predictions for A_{LL} based on different gluon polarization scenarios. The fragmentation functions for π^+ and π^- are based on the KKP fragmentation functions [37]. This first measurement of A_{LL} for charged pion production disfavors a large gluon polarization scenario. Several systematic checks have been performed. The leading systematic uncertainty is due to the bias introduced by the trigger used for this analysis. This trigger is based on a jet patch trigger, which introduces a bias

towards jets with a large fraction of neutral energy. The impact of this trigger on the charge pion asymmetry analysis has been estimated using a MC sample. This uncertainty amounts to approximately 5×10^{-3}, which is comparable to the statistical uncertainty of the first p_T bin. In addition, asymmetries were calculated for trigger-jets in comparison to away-side jets. Both asymmetries have been found to be consistent within statistical uncertainties.

A proof-of-principle measurement of the longitudinal spin transfer D_{LL} in inclusive Λ ($\Lambda \rightarrow p\pi^-$) and $\overline{\Lambda}$ ($\overline{\Lambda} \rightarrow p\pi^+$) production in polarized proton-proton collisions at a center-of-mass energy of 500 GeV has also been carried out by STAR. The hyperons measured in this study had a mean transverse momentum (p_T) of about 1.3 GeV/c and a longitudinal momentum fraction of $x_F = 7.5 \times 10^{-3}$. The measurement of D_{LL} for inclusive Λ and $\overline{\Lambda}$ production may provide constraints on strange (anti) quark polarization [38] and can yield new insight into polarized fragmentation functions [39]. The extension of the p_T region to large values is essential.

The STAR preliminary results of the measurement of the longitudinal double-spin asymmetry A_{LL} for inclusive jet production [16] is shown in Figure 13 as a function of p_T for $5 < p_T < 30$ GeV/c in comparison to several gluon polarization scenarios as described earlier. Jets are reconstructed using a midpoint cone clustering algorithm using a cone radius of 0.4. This algorithm is fed in the case of STAR by reconstructed electromagnetic clusters in the STAR BEMC and tracks from the STAR TPC. The uncertainties show statistical uncertainties only. Various systematic effects have been
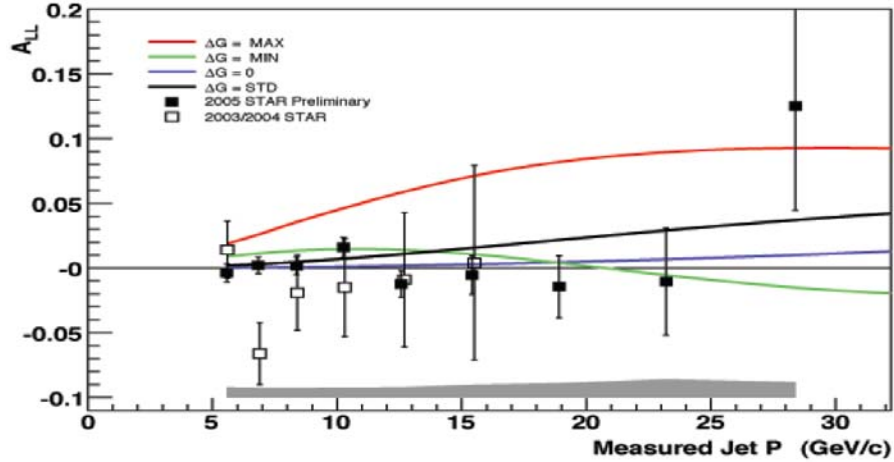
Figure 13: Preliminary longitudinal double-spin asymmetry A_{LL} for inclusive jet production at $\sqrt{s} = 200\,\mathrm{GeV}$ as a function of p_T $(0.2 < \eta < 0.8)$ for Run 5 in comparison to several gluon polarization scenarios and the 2003/2004 published data.

studied. The dominant contributions to the systematic uncertainties result from false asymmetries, trigger bias and jet reconstruction bias. The 2005 A_{LL} inclusive jet

measurement is found to be in good agreement with the previous 2003/2004 measurement. The current measurement extends the p_T region to larger values, where the quark-gluon contribution starts to become important. This analysis rules out most GRSV fits with ΔG much larger than the GRSV std. solution. It provides the most precise A_{LL} measurement to date to constrain the gluon polarization of the proton at RHIC.

Taking all current PHENIX and STAR A_{LL} measurements together in comparison to different NLO perturbative QCD predictions for A_{LL} yields a consistent picture which rules out a large gluon polarization scenario. The STAR inclusive measurements will benefit enormously from the increased data sample in Run 6 due to increased beam polarization, increased integrated luminosity, and the wider detector acceptance at central rapidity with the completion of the STAR BEMC. The expected statistical errors on the inclusive jet measurement for 2006 are shown in Fig. 14. In addition to the great
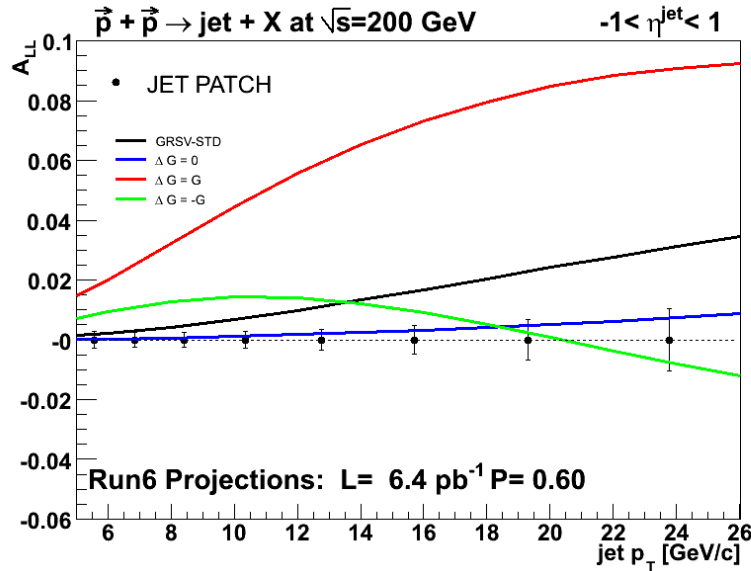

Figure 14: Projected statistical errors for inclusive jet A_{LL} based on the number of jet patch triggers taken in the second period of 2006 longitudinal pp running.

improvement in inclusive jet statistics in 2006, STAR collected significant samples of di-jets. This will allow a better constraint of the underlying event kinematics to extract the shape of the gluon polarization in a global analysis [40]. Photon-jet coincidence measurements are expected to provide a theoretically clean way to extract the polarized gluon distribution. The 2006 data set will contain a first look at this channel to be used to fine tune triggers and cuts for the upcoming run. High quality photon-jet measurements at both $\sqrt{s} = 200\,\text{GeV}$ and 500 GeV are essential to maximize the kinematic coverage in x as well as to provide a means to measure the effect of scaling violations at fixed Bjorken-x, but with different p_T values. Completing these 200 GeV measurements is the primary goal for the next two years of pp collisions.

2.3 Transverse polarized proton-proton running in FY08-FY10

The study of transverse spin effects at forward rapidity will continue to play an important role for the STAR spin physics program. An adequate amount of running time devoted to transverse polarized proton-proton collisions during the upcoming polarized proton-proton runs in FY08 - FY10 will be critical. The exact split between longitudinal and transverse data taking at STAR is still subject to ongoing discussions and has to be quantified in more detail over the next couple of months.

The beam-use request for FY08 and FY09 by the STAR collaboration to operate RHIC at 200GeV center-of-mass energies in polarized proton-proton collisions will allow STAR to complete fundamentally new measurements, which are unique to its detector capabilities, in particular, with the completion of the STAR Forward-Meson Spectrometer (FMS). The STAR FMS is a 2m square wall built from 1264 individual lead glass detectors. It is mounted 706 cm west of the STAR interaction point, spanning $\sim 2.5 < \eta < 4$ with full azimuthal coverage. State of the art analog to digital converters and field-programmable gate arrays will provide exceptional detection capabilities for large rapidity neutral meson and direct photon production, and for particle correlation studies spanning large rapidity intervals. Triggering and energy measurements of large rapidity electron and positron production are also possible. The FMS together with the existing STAR calorimeter system will allow for wide coverage in η ($-1 < \eta < 4$).

The large pseudo-rapidity coverage of the STAR calorimeters will afford important new measurements involving correlations of identified hadrons and photons at mid-rapidity and forward rapidity as well as continued study of large spin effects in particle production at forward rapidity that have been pioneered by the STAR collaboration. The measurement of large transverse single-spin asymmetries by the STAR collaboration has received a lot of attention in recent years. The theory community has been highly stimulated by the observation of large spin effects at forward rapidity in transverse polarized proton-proton collisions, whose understanding constitutes one of the most challenging problems in QCD. We know that inclusive pion production has large, x_F dependent transverse single spin asymmetries within the acceptance of the FMS. The large acceptance of the FMS will permit separation of spin-dependent fragmentation contributions (Collins effect) from the contributions arising from correlations between the proton spin and initial-state partonic transverse momentum (Sivers effect) via the measurement of transverse spin dependence of neutral pion pairs from a fragmenting parton. A recent paper [41] on transverse single-spin asymmetries in photon-jet measurements points out unique opportunities for the kinematical regime of large and positive photon pseudo-rapidities and negative jet pseudo-rapidities. It has been shown that predictions for the asymmetry in terms of gluonic-pole cross-sections in pQCD can be confronted with expectations within the framework of generalized parton model, involving standard partonic cross-sections. Measurements for photon-jet measurements will allow STAR to further enhance the understanding of transverse single-spin asymmetries. The request for transverse polarized proton-proton running in FY10 will allow STAR to probe the scale dependence of various measurements involving large

transverse spin asymmetries. It is essential that these measurements are performed utilizing the unique detector capabilities and acceptance of STAR.

2.4   Spin physics beam use requirements to complete 200 GeV ΔG(x) measurements

STAR's spin physics goals for $\sqrt{s} = 200\,\text{GeV}$ remain focused on the primary goal of mapping the gluon polarization in a polarized proton as a function of Bjorken x. Toward this end, we feel that 80 pb^{-1} of recorded luminosity (with polarization near the design goal of 70%) split between two long pp runs—one in each of the next 2 years—are needed to provide the desired experimental uncertainties. We anticipate that STAR's DAQ1000 upgrade will be in place for the 2009 run, enhancing trigger bandwidth and reducing the dead time for pp data collection, thus providing the final step needed to complete this high priority measurement. In addition, forward tracking upgrades necessary for efficient use of the 500 GeV beam for the W physics program will not be available until after the 2009 run.

Significant improvements to the constraints on ΔG(x) over the data we have already collected in 2006 will most likely come from the following sources: (1) improving the statistical precision for high-p_T (15-30 GeV/c) inclusive jets; (2) collecting a statistically meaningful sample of photon-jet coincidences, providing event-by-event information on the Bjorken x-values of the colliding partons, coupled with leading-order dominance of quark-gluon interactions; (3) di-jet coincidences, which will give better statistical sensitivity than photon-jet coincidences, but less constrained parton kinematic information (the ratio x_1/x_2 for the two colliding partons should be well determined, but resolution on p_T, hence x, absolute scales will be coarse). Along the way toward these goals, we may also extract inclusive direct photon asymmetries, but these will never compete statistically with inclusive jet production, and are likely to provide only a somewhat coarse crosscheck on the pQCD analyses. As STAR has always argued, photon-jet coincidences provide better sensitivity to ΔG(x) than inclusive photon asymmetries, despite giving a smaller total event sample, because the possibility to extract initial-state parton kinematic information permits emphasizing events in regions of phase space that involve both sizable quark polarizations and large parton-level two-spin asymmetries. Future STAR pp runs will devote most of the limited available trigger bandwidth to photon and coincidence triggers; but the optimal mix of these triggers will be dictated by data analysis results from Run 6 still in progress.

Among the most important issues under investigation in analyzing 2006 data are the following:

Evaluation of γ-jet and jet-jet sensitivity to ΔG(x):   The interpretation of A_{LL} data for inclusive channels is subject to model-dependence regarding the assumed shape of ΔG(x), since different p_T bins integrate over broad, and substantially overlapping, x-ranges. Photon-jet and di-jet coincidences offer complementary strengths in reducing this model-dependence. The former is kinematically preferred because the resolution attainable on p_T, hence on x, is far better for photons than for jets. But attaining a statistically sufficient photon-jet data set with realistic integrated luminosities will be challenging. Since both

channels have demanded new analyses, we do not yet have clear demonstrations of their anticipated sensitivity levels, and so cannot yet provide the optimized trigger compromise that will be needed to accommodate both within the limited trigger bandwidth.

One physics source for the complementarity between the two channels is illustrated in Figure 15, which plots a leading-order parton-level statistical "figure of merit" for ΔG sensitivity, defined as the product of the invariant amplitude squared and the partonic $\hat{a}_{LL}^2$, for $qg \to qg$ and $qg \to q\gamma$ as a function of the partonic c.m. angle $\theta*$. The plot assumes that parton scattering at both $\pm \cos\theta*$ contributes incoherently to the observed coincidences at given pseudorapidities $\eta_{1,2}$. This is valid for di-jets because it is difficult in practice (though possible in principle) to distinguish quark from gluon jets. In the Compton scattering case, the photon can of course be distinguished from the quark jet, and an effective discrimination between forward and backward scattering is then provided by the quark vs. gluon distribution functions for some regions of phase space.

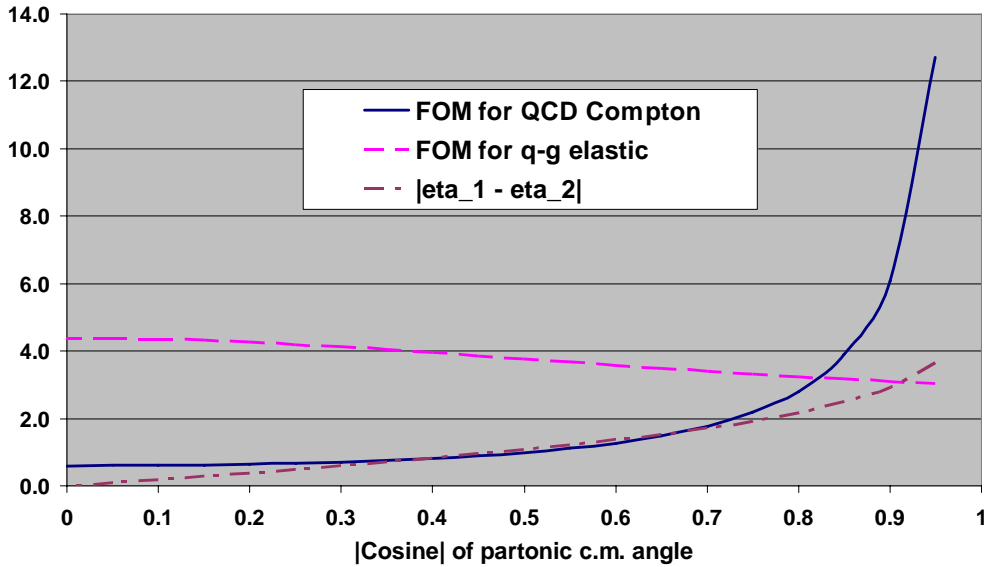**LO Statistical FOM for Photon-Jet and Jet-Jet Coincidences**

Figure 15: LO pQCD parton-level figure of merit (defined as $\overline{|\mathrm{M}|^2}\hat{a}_{LL}^2$) for QCD Compton scattering (solid curve) and quark-gluon elastic scattering (dashed curve). The squared amplitude is taken as the sum, and $\hat{a}_{LL}$ as the weighted average, of values at $\pm \cos\theta*$. The dot-dashed curve is the kinematic relation $|\eta_1 - \eta_2| = 2\tanh^{-1}(\cos\theta*)$.

But in any case, the photon production sensitivity is optimized at far backward c.m. angles ($|\cos\theta^*|\approx 1$ in the figure) by peaks in both cross section and spin asymmetry. In contrast, the presence of a *t*-channel gluon-exchange pole for the *qg* elastic scattering couples a strong forward peak in the cross section with very small spin sensitivity, leading to a modest θ^* dependence of the figure of merit, with a maximum at 90°. As also illustrated in the figure, these different sensitivities imply that photon-jet coincidences are most powerful for $|\eta_1 - \eta_2| > \approx 2$, while di-jet coincidences favor smaller values. In both cases, one is most interested in asymmetric partonic collisions, $|\eta_1 + \eta_2| = |\ln(x_1/x_2)| > \approx 1$, in order to probe low-*x* gluons with high-*x* (hence highly polarized) quarks. With the FMS, STAR's coverage will extend over -1 $\leq \eta \leq$ 4, providing an outstanding opportunity to map $\Delta G(x)$.

The curves in Figure 15 do not take into account the factor $e_q^2 \alpha_{em} / \alpha_s \ll 1$ that appears in the ratio of cross sections for the semi-electromagnetic to strong processes. In practice, at anticipated luminosities, we are likely to fill much of the bandwidth with triggers for either process. Thus, a critical aspect of the comparison is the fraction of triggers that lead to desired reconstructable coincidence events in each case. These fractions are influenced by physics – *e.g.*, the fraction of di-jet events arising from qg scattering under given kinematic conditions – but also depend on technical issues that are being quantitatively assessed for realistic detector performance in the analysis of 2006 data and related simulations: (1) What levels of γ retention and π^0 rejection can be attained to optimize signal/background for photon-jet coincidences? (2) How low in p_T can direct photons be identified in the presence of a growing π^0 background? (3) Does low-mass background seen to date in π^0 reconstructions in STAR constitute an additional background for direct photon analyses? (4) Is an L2 coincidence trigger for γ-jet desirable, or will it enhance background more than signal? (5) How efficiently, and with what bias in extracted four-momenta, can jets be reconstructed beyond the barrel EMC region, despite the services gap (η=0.98 − 1.08) and rapidly decreasing TPC tracking performance? (6) What trigger biases on contributing partonic processes and *x*-ranges are imposed by the 2006 di-jet trigger?

By the time of Run 8 STAR will be better able to demonstrate the sensitivity to $\Delta G(x)$ attainable in given length runs at 200 GeV with an optimized trigger mix. At this time we anticipate needing approximately 80 pb^{-1} of pp collision to complete the current 200GeV $\Delta G(x)$ program. Assuming the middle of the CAD projections for performance in the coming years and data taking efficiency in the second year from DAQ1000 the time requested, 12+2 weeks in 2008 and 14+2 weeks in 2009, should be sufficient and should allow for a moderate amount of transverse running as well.

With the completion of the FMS during run 7, the STAR detector has nearly continuous electromagnetic calorimetry for -1 < η < +4. With this calorimetry, STAR will be uniquely positioned to measure the correlation between transverse spin and relative transverse momentum as determined by observing either pairs of jets or pairs of hadrons. The back-to-back di-jet asymmetry studies can be extended to span larger η, including

the range in which sizable transverse SSA are observed for inclusive $\tilde{\pi}$ production. The larger η measurements will isolate the quark Sivers distribution. The transverse spin dependence of near-side di-hadron correlations can be used to probe for non-zero transversity through the Collins effect. The original estimates were that data samples with ~70% beam polarization and 30 pb^{-1} of integrated luminosity would be required to gain sensitivity to transversity in di-hadron measurements at STAR. Data samples of this magnitude will also provide access to transverse SSA for inclusive photon production. It is anticipated that polarized proton collisions at √s = 200 GeV in Runs 8 and 9 will attain the luminosity and polarization goals stated for the RHIC spin program. In developing the *Research Plan for Spin Physics at RHIC* [42], it was assumed that approximately 25% of the polarized proton collision time would be spent with transverse polarization. A data sample recorded with only the STAR calorimeters, corresponding to 30 pb^{-1} sampled, could be achieved in several weeks of running at full luminosity.

In summary, an optimal pp run plan for the STAR spin physics program divides roughly 30 weeks of collision time between 2008 and 2009. The time will be devoted primarily to longitudinal spin running at $\sqrt{s} = 200$ GeV but would allow for modest amounts of transverse running as well. These runs would allow a significant map of the *x*-dependence of the gluon polarization, within the approximate range $0.03 < x < 0.3$. Smaller values of *x* would be subsequently probed in 500 GeV running. We continue to support 500 GeV beam development provided the physics goals are met. In addition, we strongly support continued polarization development of proton beams in the AGS, in parallel with RHIC stores.

2.5 Spin physics beam use proposal for Run 8

The STAR Collaboration proposes a polarized p+p run of (12+2) weeks. The major goal for this run is to make significant progress towards mapping out the spin-dependent gluon distribution of the proton, ΔG(*x*). The geometric mean of the CAD's projections for Run 8 indicate that 95 pb^{-1} (range of 55-135 pb^{-1}) could be delivered in 12 weeks of running time. Experience indicates that with that amount of integrated luminosity delivered to the detector, STAR could record over 30 pb^{-1}, or ~ 1/3 of the necessary 80 pb^{-1}. Analysis needed to fully understand the optimum trigger mix, to adjust the weighting between di-jet and γ-jet events, and estimate final statistics is still under way. With this amount of beam delivered and recorded it is expected that a moderate amount of running time can also be devoted to the transverse program as well. Final determination of the optimum balance between transverse and longitudinal running awaits quantitative projections for the physics measurements to be carried out.

3. Forward Tagged Proton Studies in STAR

3.1 Polarized proton-proton elastic scattering (p$^\uparrow$p$^\uparrow$ → pp)

As part of its scientific program, the STAR Collaboration proposes to investigate the non-perturbative regime of QCD using polarized proton beams at RHIC, the STAR detector

and the Roman Pots of the pp2pp experiment [43-45]. The pp2pp Roman Pot detectors will be used to tag very forward protons, thus selecting processes in which the proton stays intact, and the exchange has quantum numbers of the vacuum,—so called Pomeron (IP) exchange. For these events, the probability of measuring reactions where colorless gluonic matter dominates the exchange is enhanced. The use of polarized proton beams, unique at RHIC, will allow exploring unknown spin dependence of diffraction including both elastic (Fig. 16) and inelastic processes (Fig. 17). As the entire energy range of this proposal has been inaccessible to proton-proton (elastic) scattering in the past, new results of high quality will be produced. A more detailed description of the physics can be found in [46-48].

3.1.1 Spin averaged observables

The measurement of the differential pp cross section $d\sigma/dt$ over the extended t-range will include the region at lower |t| that is particularly sensitive to the ρ-parameter. Hence we will measure: 1) the ρ-parameter; 2) the nuclear slope parameter b in a combined fit to the differential cross section, and 3) the total cross section σ_{tot}.

One example of the interest in such studies is that an asymptotic difference observed between the differential and total cross sections for pp could indicate an Odderon contribution to the scattering amplitude. The absence of an Odderon contribution would lead to identical cross sections, the differential and total cross sections approaching each other roughly as $s^{1/2}$. The measurement of the total cross section, σ_{tot}, at the highest possible energy will also probe the prevalent assumption that the cross sections for pp and p̄p scattering are asymptotically identical.

With the expected $20 \cdot 10^{6}$ elastic events the estimated error on the slope parameter is $\Delta b = 0.31$ (GeV/c)$^{-2}$ and that for the ratio of the real to imaginary part, $\Delta\rho = 0.01$. This is comparable to the precision for existing measurements from pp and p̄p data. The $\Delta\sigma_{tot} = 2\text{-}3$ mb, where the largest contribution is from the error on the luminosity measurement.

3.1.2 Spin dependent observables

By measuring spin related asymmetries one will be able to determine elastic scattering at the amplitude level [49-51]. The availability of longitudinal polarization at STAR will allow measuring A_{LL} in addition to A_{NN}, A_{SS}, and A_{N} resulting in a significant improvement of the scientific reach of these measurements. Full azimuthal coverage of the elastic events that we are planning to have will assure high efficiency and small errors in the measurements.
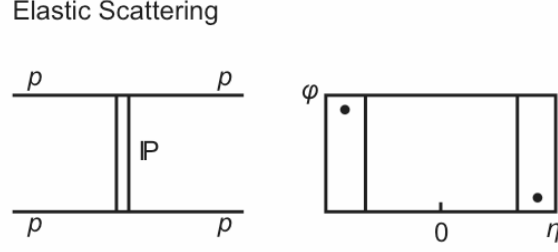
Fig. 16. Diagram of the elastic scattering process in the t-channel.

One of the physics motivations to measure A_N is the possibility of the rise with energy of the spin-flip to spin-nonflip amplitudes ratio. In other words it may occur that the small contribution from hadronic spin-flip to the spin single-spin asymmetry measured with a polarized jet target at 100 GeV/c could be increased at $\sqrt{s}$=200 GeV. This study will help to address the long standing problem of the energy dependence of the spin flip amplitude, which remains a question for experiment at present.

Reaching such a small |t|-value allows measuring the single spin analyzing power A_N close to its maximum at |t| =0.0024 $(GeV/c)^2$, where A_{max} = 0.04, at $\sqrt{s}$ = 200 GeV. The A_N and its t-dependence in the covered range are sensitive to a possible contribution of the single spin-flip amplitude, ϕ_5, from the interference between the hadronic spin-flip amplitude with the electromagnetic non-flip amplitude.

An additional contribution of the hypothetical Odderon to the pp scattering amplitude can be probed by measuring the double spin-flip asymmetry, A_{NN} [52]. The calculation in [52] shows that A_{NN} is sensitive to contributions of the real and imaginary parts to the double spin-flip amplitude, ϕ_2, in the range 0.003 < |t| < 0.010 $(GeV/c)^2$. At a higher value of |t| the difference between a pure Pomeron contribution and an equal mixture of Pomeron and Odderon at the five percent level are hard to distinguish, while a pure Odderon contribution would lead to a very small double spin-flip asymmetry.

The useful interval with 100% acceptance for elastic scattering is 0.003 < |t| < 0.024. Given polarization of 60%, and 2.3mb cross section within our acceptance, we estimate that we will obtain $20 \cdot 10^6$ events. If the data are distributed into four t subintervals, this results in $5 \cdot 10^6$ events in each. The corresponding errors are δAn=0.0017, δA_{NN}=δA_{SS}=0.003.

3.2 Diffractive processes pp $\rightarrow$ p + X + p

In the double Pomeron exchange process each proton "emits" a Pomeron and the two Pomerons interact producing a massive system M_X. The massive system could form resonances or consist of jet pairs. Because of the constraints provided by the double Pomeron interaction, states coupling preferentially to gluons will be produced with much reduced backgrounds compared to standard hadronic production processes.

The gluonic processes (IP exchanges) begin to dominate when the rapidity gap between the forward protons and the system produced at center rapidity is $\Delta y > 3$. This is achieved at RHIC with masses M_X up to 10 GeV. The STAR detector at RHIC equipped with Roman Pots is ideally suited for studying processes where the M_X decays solely into charged particles. In addition one can study processes at RHIC with leading high p_T particles at central rapidity, which are equivalent to jet studies.

3.2.1 Central production through double Pomeron exchange (DPE) process.

The above processes are commonly characterized by using variables t, ξ and M_X, where t is four-momentum transfer between the incoming and outgoing protons, $\xi = \Delta p/p$ is the momentum fraction carried off by the Pomeron and M_X is invariant mass of the produced system. In case of double Pomeron exchange, separate t and ξ variables exist for each proton-Pomeron vertex.

Tagging and measuring forward protons is important since it removes the ambiguity of a (complementary) rapidity gap tag, which has a background due to the low multiplicity of diffractive events, and allows the full characterization of the event in terms of t, ξ and M_X.
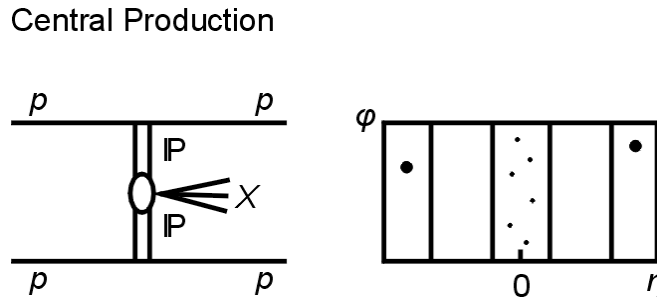
Central Production

Fig. 17. Diagram of the Central Production (DPE) process in the t-channel

3.2.2 Hard and Soft Diffraction

The strength of the STAR detector—excellent charged particle identification and p_T resolution in the central rapidity region—coupled with ability to tag diffractive events with the forward protons with Roman pots, allows for the measurement of single particle spectra as a function of t and ξ of the outgoing proton. STAR has established that using the leading particle, with highest p_T, one can characterize jet like phenomena in hadron-hadron collisions.

3.2.3 Central production of glueballs

The idea that the production of glueballs is enhanced in the central region in the process $pp \rightarrow pM_Xp$ was first proposed by [53] and was demonstrated experimentally [54]. The crucial argument here is that the pattern of resonances produced in the central region, where both forward protons are tagged, depends on the vector difference of the transverse momentum of the final state protons $\bar{k}_{T1}$, $\bar{k}_{T2}$, with $dP_T \equiv | \bar{k}_{T1} - \bar{k}_{T2} |$. The so-called dP_T filter argument is that when dP_T is large ($\geq \Lambda_{QCD}$) $\bar{q}q$ states are prominent and when dP_T is small, the surviving resonances include glueball candidates [52],[53].

STAR has studied the geometrical acceptance of the proposed setup for both SDD and DPE processes, generating protons with t and ξ uniformly distributed in the regions $0.003 < |t| < 0.04$ and $0.005 < \xi < 0.05$ respectively. It was assumed that the Roman Pots (RPs) are at least 12σ of the beam size at the detection point. The plot in Fig. 18 shows acceptance as function of M_X, the red dots indicating the location of the Roman Pots.
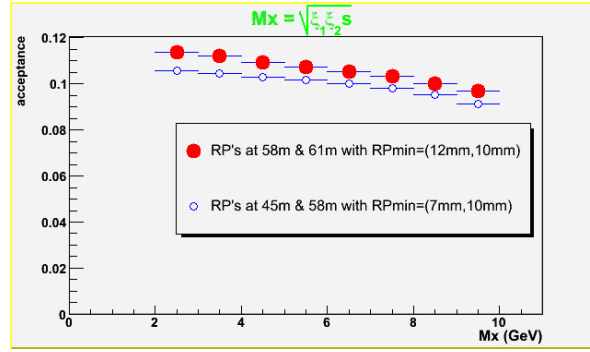

Fig. 18 Mass geometrical acceptance for DPE processes, red dots.

We conclude that there is good acceptance to measure inelastic diffraction DPE with β^*=20m. So while taking elastic data, a fraction of the trigger band-width could be dedicated to include events with two or one proton in the forward direction.

In the proposed research, large data samples of diffractive states can be obtained and analyzed as a function of diffractive mass and t ($d^2\sigma/dM_X^2dt$) for central production. As noted above, when dP_T between two out going protons is small, the fraction of glueball candidates is enhanced; when the dP_T is big the qqbar states are enhanced. In quantifying the threshold between these regimes, the WA102 experiment [54] found "small" to be $dP_T < 0.2$ GeV and "big" to be $dP_T > 0.5$ GeV.

With the expected luminosity one can collect about 450,000 triggered DPE events during the three days of running, with 40 hrs of useful beam time. One assumes a 10 μbarn cross section within our acceptance for the DPE process, where it is required that two RPs on each side are used allowing reconstruction of the outgoing proton momentum. The number of events for which only one proton tag is used is factor of 4-5 higher.

The search for glueballs remains an experimental question and the proposed research will add significantly to the world body of knowledge concerning their possible existence.

3.3 Forward tagged proton implementation plan

The pp2pp Roman pots mounted on the outgoing beams, down stream from the STAR detector shall be used as shown in Fig. 19. To achieve full azimuthal coverage for elastic events, at each location one Roman Pot station is horizontal and one vertical. RHIC accelerator magnets are used for momentum analysis resulting in forward proton taggers installed in the warm straight section between Q3 and Q4 magnets. The pp2pp Roman Pots are a moveable detector system allowing approach to the beam as closely as possible, thus extending the t and ξ ranges to the lowest values.
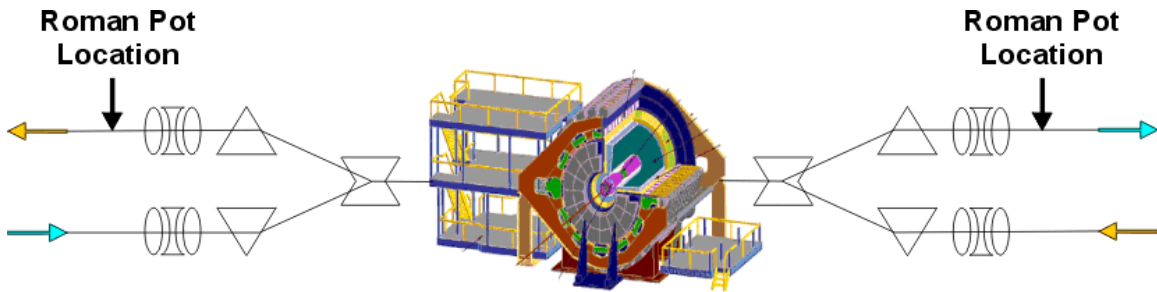

Fig. 19. The Roman pots of the pp2pp experiment in the STAR interaction region, with the arrows indicating proposed location. At each location one Roman Pot station is horizontal and one vertical.

3.4 Forward tagged proton beam use request

To maximize physics output, several days of efficient data taking are needed. The main reason is that in order to reach the t and ξ values needed for both diffractive and elastic data, beam scraping and special optics are needed. Hence, taking into account machine and detector uptime we are requesting ~3 days of dedicated running with polarized protons in Run 8 and Run 9.

Using the capacity of existing power supplies optics of $\beta^* = 20$ m at $\sqrt{s} = 200$ GeV can be produced allowing the t coverage with 100% acceptance for elastic scattering for $0.003 < |t| < 0.024$. The setup time of the $\beta^*=20$ m optics is estimated by the C-AD to be 12 - 24 hours, leaving the remaining time for dedicated data taking.

3.5 Integration of pp2pp DAQ and trigger with STAR

The essential parts of the pp2pp DAQ system, both hardware and software, will remain unchanged and can be easily integrated into the STAR-DAQ framework. The current pp2pp DAQ was written as a detector extension to STAR. The pp2pp core DAQ system, Run Control, Data Monitoring & Online Q&A histograms are all exactly the same as in STAR-DAQ and as such can be easily integrated into STAR DAQ.

The STAR-pp2pp DAQ also retains the possibility of running pp2pp in a contained standalone fashion, which would allow pp2pp to test and debug its equipment without interference with STAR. It would also allow pp2pp to take data decoupled from STAR in the same manner as it did while it was at IP2, if the need arises.

The current pp2pp trigger is based on coincidences of a small number of (16) signals from scintillators, which can be adapted to the STAR CDB/DSM trigger scheme with only one pair of CDB/DSM STAR Trigger boards. Such a system is conceptually equivalent to many of STAR Trigger detectors (i.e. CTB, ZDC) and should not be a problem.

Once this has been done an opportunity naturally presents itself to run pp2pp's Roman Pots together with STAR central rapidity (or any other) detectors to enhance the inelastic physics program. At the same time the elastic physics can be run in parallel with only the Roman Pots being read out at a higher rate, in the so called "fast detectors only" mode.

In summary the physics program with tagged forward protons at STAR will:

1. Study elastic scattering and its spin dependence in unexplored t and √s range;
2. Study the structure of color singlet exchange in the non-perturbative regime of QCD;
3. Search for diffractive production of light and massive systems in double Pomeron exchange process;
4. Search for new physics, including glueballs and Odderon.

The proposed studies will add to the world body of knowledge concerning QCD in the non-perturbative regime where calculations are not easy and one has to be guided by measurements. In this way the proposed program extends the physics reach of both STAR and RHIC.

4.0 Modifications to the STAR Detector configuration for Run 8

A significant modification to the STAR Detector leading up to Run 8 will be the removal of the STAR Silicon Vertex Tracker and Silicon Strip Detector after Run 7. This modification will be made to provide space for future tracking upgrades and to allow for

reconfiguration of the SSD following the completion of the physics mission of the SVT. Among other things, the "near zero mass" interior configuration of STAR prior to installation of the mid-rapidity tracking upgrades will provide a unique opportunity for cross-checks of systematic uncertainties in the measurement of non-photonic electrons.

Another important upgrade will be continued refinement of the STAR Vertex Position Detector (VPD) to improve event selection at trigger Level 0, so that fewer events are rejected in offline analysis.

New physics reach essential to the physics goals of Run 8 will be provided by the newly commissioned Forward Meson Spectrometer.

The STAR Forward Meson Spectrometer consists of lead glass detectors in a hermetic stack positioned 750 cm from the interaction point (Fig. 6). The inner calorimeter is built from 476 detectors obtained from IHEP, Protvino. Each lead-glass bar of the inner calorimeter has dimensions of 3.8cm × 3.8cm × 45 cm corresponding to 18 radiation lengths. These detectors are stacked into a 24 × 24 matrix having a central 10 × 10 element hole for the beams. The outer calorimeter is built from 788 detectors built from Schott F2 glass obtained from FermiLab. Each lead-glass bar of the outer calorimeter has dimensions of 5.8cm × 5.8cm × 60 cm and also corresponds to 18 radiation lengths. They are stacked into a 34 × 34 matrix with a central 16 × 16 element hole into which the inner calorimeter fits. The FMS is positioned west of STAR on a platform extension of the tunnel entrance into the Wide Angle Hall. Its distance from the interaction point is limited by the DX magnet to the west of STAR. The FMS views reaction products from the colliding beams through the hole in the STAR magnet poletip and will face the oncoming deuteron beam in d+Au collisions. The FMS spans the full azimuth for $2.5 < \eta < 4.0$. The addition of the FMS will provide STAR with nearly contiguous electromagnetic calorimetry, including the barrel and endcap EMC, spanning the full azimuth for the rapidity range $-1 < \eta < +4$. Smaller matrices of the 3.8cm × 3.8cm cross section IHEP, Protvino detectors have been operated since RHIC Run 2 in the modular STAR Forward Pion Detector.

The 1264 detectors of the FMS are housed in enclosure halves mounted on the north and south sides of the vacuum pipe. A rail system on the tunnel extension platform allows the enclosure halves to be moved away from the beam pipe for servicing the vacuum system at the STAR interaction point.

Cerenkov photons from showers in the lead glass are detected by FEU-84 photomultiplier tubes powered by resistive voltage dividers. Given the distance from the interaction point, single photons can be resolved from pairs of photons produced in the decay of neutral pions for energies up to 60 GeV.

To limit the dissipated power, the FEU-84 that will be used in the FMS will be powered by a Cockcroft-Walton (CW) base that has been designed and built at Penn State University. Extensive tests performed indicate the stability and linearity of their CW design exceeds that of the resistive dividers that have been previously used.

Readout of the FMS detectors will be performed using 12-bit analog-to-digitial converters (ADC) that have been developed at the University of California, Berkeley / Space Sciences Institute. A 32-channel 9U VME prototype board has been produced and is undergoing final tests. The ADC are clocked at 9.38 MHz and present their data to on-board field-programmable gate arrays for readout and bit manipulations as an interface to the STAR trigger system. Each board presents 32 bits of information every 107 ns to a tree of data storage and manipulation (DSM) boards for triggering on either large energy deposition in single detectors (high towers) or on large energy sums observed in the FMS.

The construction of the FMS is expected to be fully commissioned in Run 7 and ready for Run 8.

5. Recent heavy ion physics results and beam use proposal for Run 9

5.1 Recent relativistic heavy ion physics results

Analysis of the Au+Au data from run 4 and the Cu+Cu data from run 5 are ongoing, as well as analysis of the baseline p+p datasets from Runs 2 through 6. The research on these data is becoming increasingly sophisticated, as shown for example by recent results presented at Quark Matter 2006. Specifically, the full capabilities of STAR for particle identification have been utilized to measure identified particle spectra out to high p_T (~12 GeV/c), while the large acceptance of STAR has enabled advanced analyses of correlations and fluctuations. These capabilities have afforded a number of first "proof-of-principle" measurements, documenting STAR's ability to take advantage of planned upgrades and increased luminosity available at RHIC II.
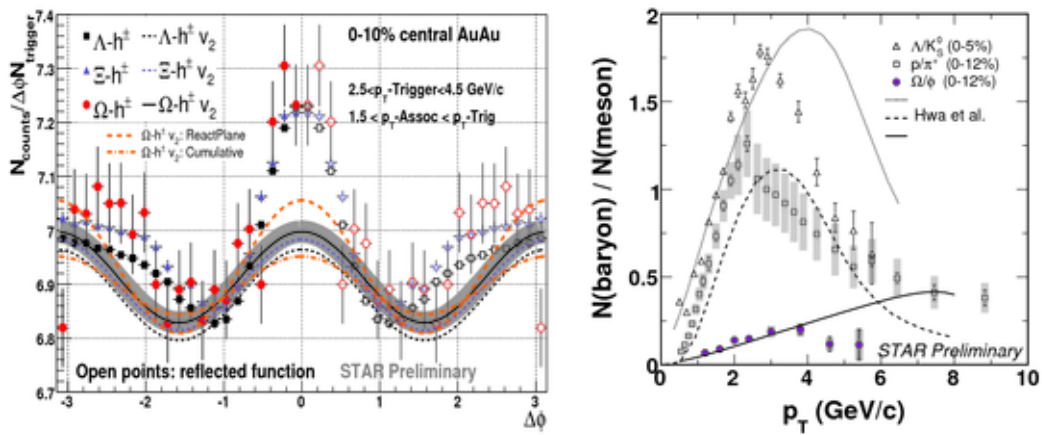

Fig. 20: Left: Hyperon-hadron $\Delta\phi$ correlations. Right: Baryon/meson ratios in central Au+Au collisions at 200 GeV. Figure from [55].

The reach of particle identification in STAR is illustrated in Fig. 20. Hyperon-hadron correlations are shown on the left; significant, and similar, correlations are seen for all species of hyperons up to and including the Omega, in apparent contradiction to predictions from a coalescence picture. Baryon to meson ratios are shown on the right; the existence of a peak in these ratios at intermediate p_T, and the increase in the location of the peak in p_T with increasing strangeness content, are predicted in a coalescence framework, but quantitative agreement between the calculation and the data is lacking. At high p_T, protons and pions are suppressed similarly in Au+Au collisions relative to their production in p+p collisions. This challenges jet quenching calculations in which, naively, protons should be more strongly suppressed due to the relatively larger contribution to their yield from gluon fragmentation.

The large values of v_2 measured in Au+Au collisions have been taken to imply that the system has an extremely small viscosity—small enough to be describable in an ideal hydrodynamic picture. In such a picture, the momentum-space anisotropy v_2 is driven by the spatial eccentricity in the initial state. In Glauber calculations of the shape of the overlap zone, this initial-state eccentricity fluctuates significantly from event to event. By measuring the fluctuations in v_2, one is sensitive to the level to which these fluctuations are preserved in the evolution of the system. Fig. 21 shows the first such measurement from STAR: v_2 is found to have large fluctuations, compatible with the fluctuations in "participant" eccentricity, indicating the extent to which v_2 is driven by the spatial orientation of the participants in the reaction relative to each other rather than to the
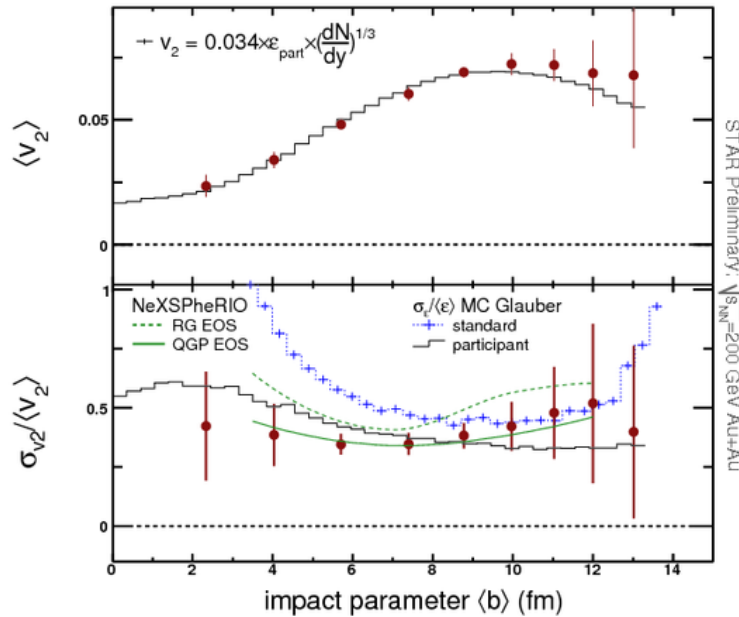

Fig. 21: Mean and relative fluctuation of v2 event-by-event. Figure from [55].

incoming impact parameter vector. A "QGP" equation of state is favored somewhat by the data, but more detailed theoretical investigation is needed in order to make strong conclusions about the sensitivity of this measurement to the details of the evolution of the system.

Correlations between a high p_T hadron and two or more other hadrons are expected to be sensitive to the reaction of the medium to the energy lost by a high energy parton which travserses it. The structure of correlations between hadrons shows large modifications in Au+Au collisions relative to the simpler, jet-like correlations seen in p+p collisions. The left panel of Fig. 22 shows the 2-dimensional correlation in $\Delta\eta - \Delta\phi$ between a high p_T trigger hadron and a lower p_T associated hadron. The near-side peak, symmetric in $\Delta\eta-\Delta\phi$ in p+p collisions, is substantially broadened in the $\Delta\eta$ direction in Au+Au collisions. Within a two-component model, the structure appears to be composed of a "jet" with properties similar to those seen in p+p collisions and a "ridge" with properties similar to those of the bulk. This "ridge" may be due to the reaction of the bulk to deposited energy. In two-particle correlations, substantial broadening is seen on the away side in $\Delta\phi$, along with a possible dip at 180 degrees in certain kinematic configurations. In order to elucidate the mechanism for this modification, a 3-particle correlation analysis has been performed, as shown in the right panel of Fig. 22. Within a two-component model, in which the "jet"-like signal sits on a flow-modulated background, off-diagonal structures are seen. These structures are consistent with conical emission as the parton traverses the medium. Future measurements with triggered datasets and particle identification over the full range in p_T will allow STAR to explore these rich correlation structures in unprecedented detail.
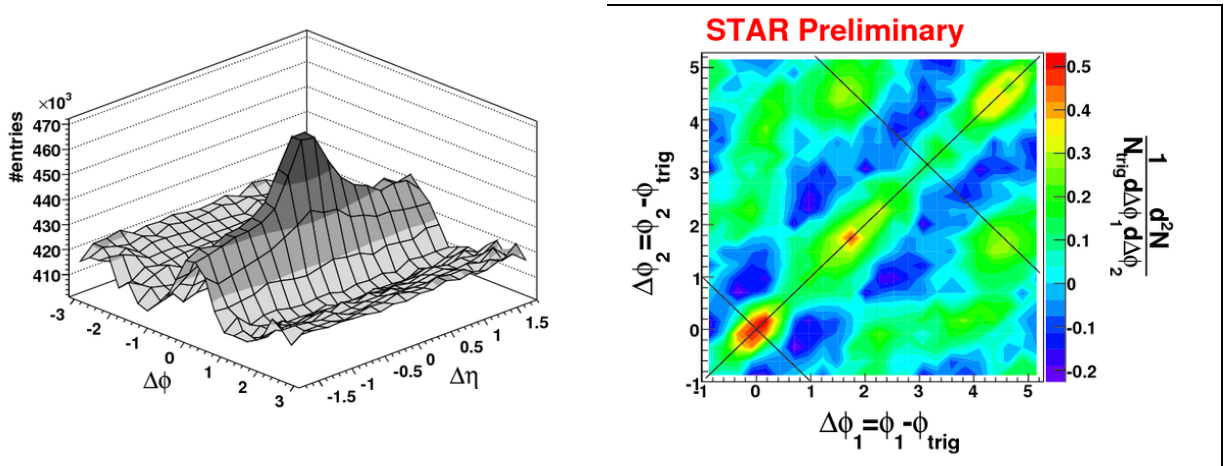

Fig. 22: Left: $\Delta\eta-\Delta\phi$ correlation in central Au+Au collision, showing an elongation along the pseudorapidity difference direction. Figure from nucl-ex/0701059. Right: correlation between two associated hadrons and a third trigger particle, where backgrounds have been subtracted using a two-component model. Figure from [55].

Unexpectedly strong suppression of non-photonic electrons has been seen in Au+Au collisions. However, the fraction of these electrons that come from decays of B mesons as opposed to D mesons remains highly uncertain. This fraction needs to be known to separate the energy loss of bottom quarks from charm quarks, since these two quark flavors are expected to lose different amounts of energy in the medium. Electron-hadron $\Delta\phi$ correlations measured in p+p collisions have been fit to a two-component model in which the measured correlation is taken to be a sum of correlations from B and D decays, the relative fraction in the sum being a parameter of the fit. The resulting fraction is shown in Fig. 23. It is consistent, within large uncertainties, with the expectation from a sophisticated Fixed Order Next to Leading Log (FONLL) perturbative QCD calculation. Additional effort to separate the relative contribution from D, B decays to the non-photonic electron spectra in Au+Au collisions is a major goal for Run 7. This will be attempted using the SVT and SSD to suppress combinatorial background. Decisive measurements of the suppression of bottom and charm separately ultimately require the Heavy Flavor Tracker and associated inner tracking upgrades.
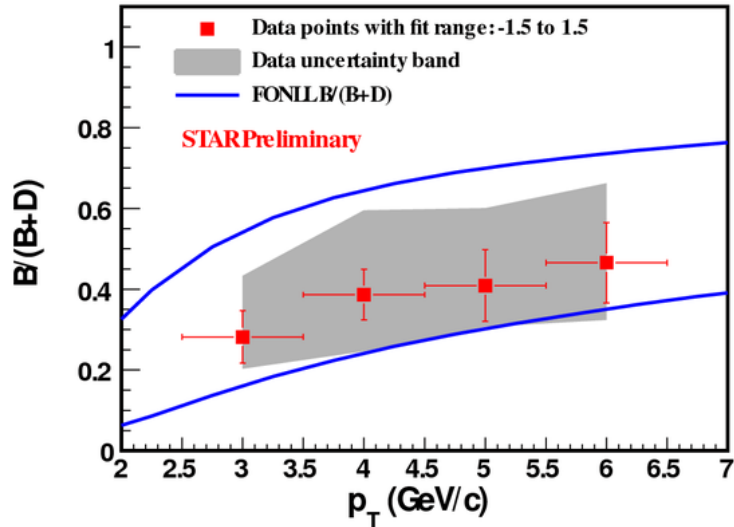

Figure 23: Relative contribution of B decays to the total sample of non-photonic electrons, from a fit of electron-hadron correlations to a two-component model. Figure from [56].

First measurements of the Upsilon cross-section in p+p collisions have been performed, through correlation of electron-positron pairs triggered using the STAR BEMC and identified using the STAR BEMC and TPC. The results are shown in Fig. 24. These first measurements will be improved in future heavy-ion and p+p runs. With the RHIC II luminosity, the precision of these measurements will be highly competitive with worldwide body of data.
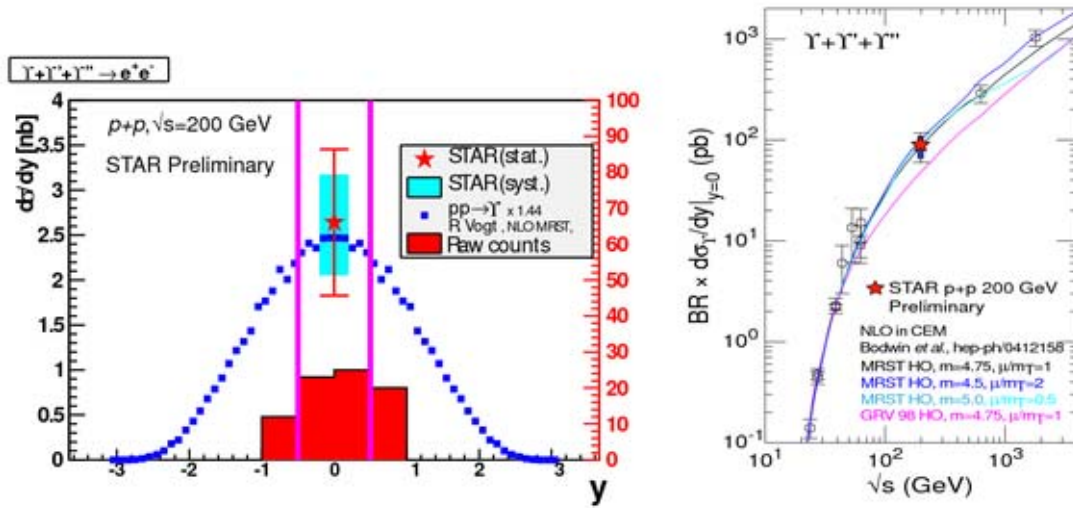
Fig. 24: Upsilon cross-section in p+p collisions at 200 GeV, as compared to world data and NLO calculations. Figure from [56].
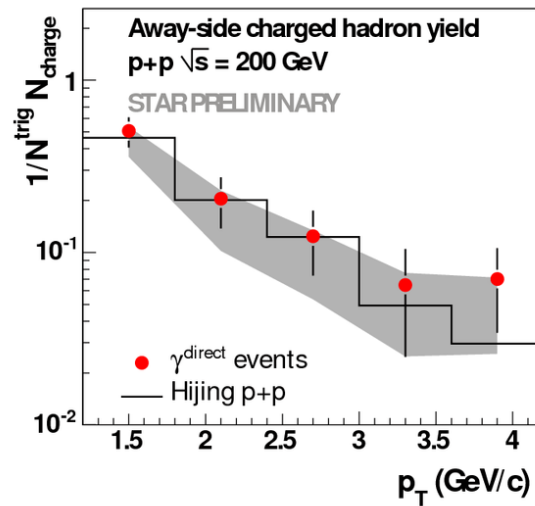

Figure 25: Spectrum of charged hadrons associated with a high p_T direct photon opposite in ϕ, in 200 GeV p+p collisions. Figure from [56].

First measurements of hadrons associated with high p_T direct photons have been performed in p+p collisions, as shown in Fig. 25. The contribution of photons from π^0 decays has been subtracted using a two-component model. Triggered photons are separated into two classes, one enriched in direct photons; the full $\Delta\phi$ correlations between hadrons and photons of these two classes are unfolded to obtain the direct

photon-hadron correlation structure. The precision of this first measurement can be improved by orders of magnitude in existing p+p datasets, and improved even further with future heavy-ion and p+p datasets. With the RHIC II luminosity the utilization of direct photons as precision probes of the dense medium will be competitive worldwide.

5.2 Au+Au beam use request for Run 9

The STAR Collaboration proposes a Au+Au run of 8+2 weeks duration at $\sqrt{s_{NN}} = 200$ GeV. A primary goal will be the utilization of the newly completed DAQ1000 upgrade and a substantial, though not fully complete, implementation of the TOF upgrade to significantly increase STAR's scientific reach in the measurement of resonances in both the hadronic and leptonic decay channels. It is anticipated that the "near zero mass" interior configuration of STAR prior to installation of the mid-rapidity tracking upgrade will result in a significant improvement in measurements of non-photonic electron spectra, v_2, and correlations with hadrons, and over the full range in invariant mass in the di-electron channel.

The low material budget in Run 9 opens the opportunity to greatly extend our measurements of non-photonic electron spectra and the v_2 of these electrons in the Au+Au environment. At high p_T the background from photon conversions in the current SVT and SSD material is approximately three times the size of the non-photonic signal, while, at low p_T, e.g. at 0.5 GeV/c, the signal to background can be as low as 1:20. While the effect of this background can be ameliorated to some extent by identifying and tracking the partner electrons of a conversion pair, when combined with combinatorial backgrounds in the Au+Au environment this conversion background produces significant uncertainties in the resulting non-photonic spectra. Minimizing such uncertainties is especially important for the measurement of v_2 and of correlations between non-photonic electrons and hadrons. With the removal of the SVT and SSD material the signal to background ratio can be improved by a significant factor. The combination of decreased material budget, the full implementation of DAQ1000 (which enables the recording of Au+Au events at 1 kHz), and the implementation of a significant fraction of the TOF upgrade will lead to a qualitative advance in leptonic measurements in STAR.

Figure 26 shows a projection of the improvement in one such measurement, the v_2 of non-photonic electrons, together with the uncertainties achievable in 9M minimum bias Au+Au events. Relative uncertainties (as indicated by the size of the vertical error bars) are reduced by almost an order of magnitude by the reduction of the material. It takes only 2.5 hours of continuous data taking to record 9M events at a recording rate of 1 kHz. Further, as shown in Figure 27, the TOF combined with the TPC provides clean identification of electrons down to very low p_T. Due to the overwhelming effect of backgrounds, to date non-photonic electron measurements have been limited in STAR to $p_T >\sim 1$ GeV/c; the removal of the material will enable full use of these cleanly identified electrons.
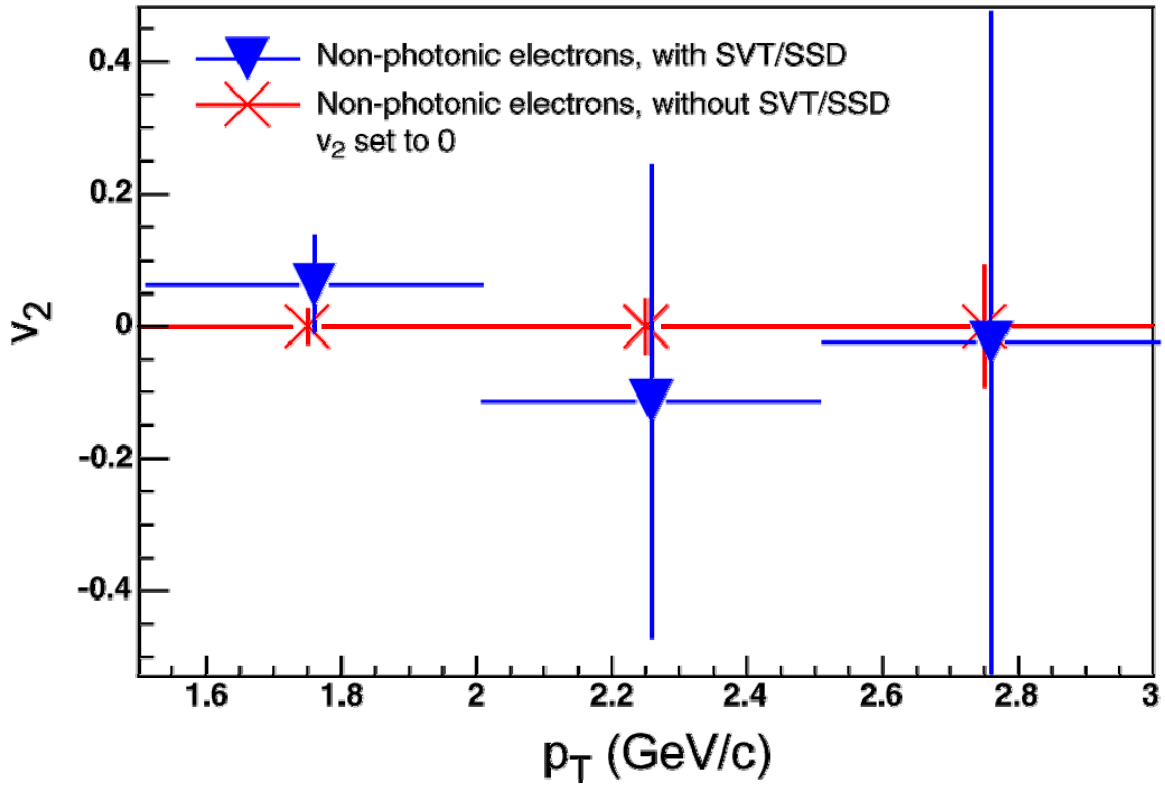
Fig. 26: Comparison between statistical significance of non-photonic electron v2 measurement with the SVT and SSD vs. without these detectors, for 9M minbias events. Figure from [57].
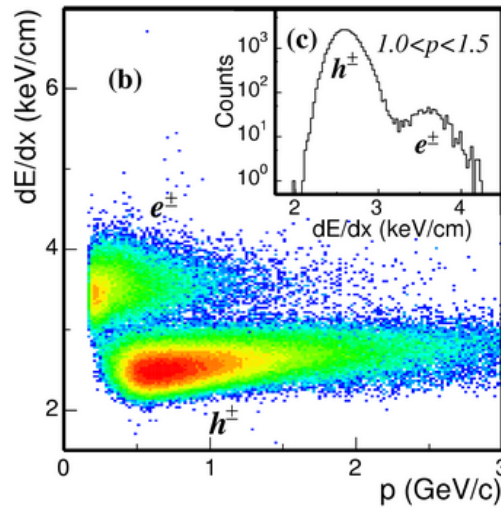

Figure 27: Electron identification capability of the STAR TOF. Figure from [58].
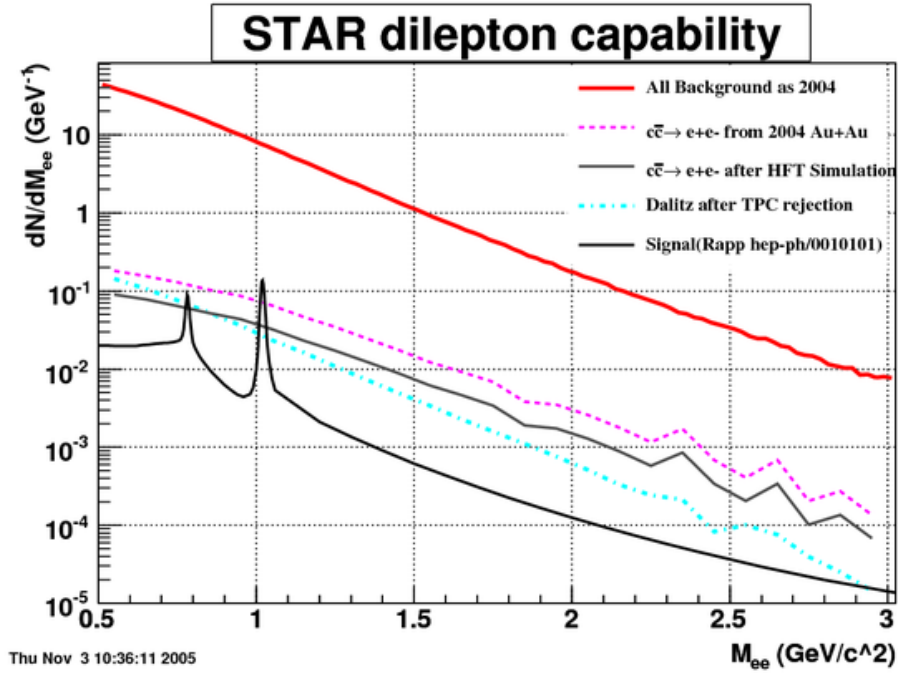
Figure 28: Dielectron invariant mass distributions for 200M central Au+Au collisions. The solid black curve is a prediction of thermal emission with STAR acceptance. The red curve at the top is the total di-electron invariant-mass spectrum with the SVT and SSD (year 2004 configuration) assuming electron PID from TOF coverage. The pink dashed line is the e+e- pair spectrum from semileptonic charm decays, the grey curve the charm e+e- spectrum after rejection using the HFT, and the blue dot-dashed line is from Dalitz decays of π^0 and η after rejection from the TPC. In the run 9 configuration, the background would consist of the sum of the blue and pink lines. Figure from the RHICII Electromagnetic Probes working group whitepaper, [59].

Another such measurement that benefits from the lack of material, DAQ1000, and the TOF is the measurement of dileptons. Figure 28 shows a projection of the dielectron invariant mass distribution within the STAR acceptance for 200M central events. The current backgrounds introduced by the SVT and SSD material are shown as the red line; with their removal, the backgrounds would be decreased substantially, and would subsequently be dominated by the irreducible background from charm, shown as the pink dashed line. The uncertainty in this background will be dominated by the uncertainty in the charm cross-section. While this measurement will be further improved with the implementation of the HFT in future runs, Run 9 will provide a significant start. At higher invariant mass, J/Psi measurements will be greatly improved by the electron identification capabilities at intermediate p_T from the TOF over a substantial fraction of the full 2π azimuth.

DAQ1000 also provides a substantial improvement for rare probes, as its pipelined architecture allows the system to run essentially without deadtime. With the current DAQ architecture, STAR tends to run with 50% deadtime, recording at 50 Hz; without

this limitation the experiment can sample approximately twice as much of the luminosity delivered by the machine. Further, with the removal of the large level of material in the support structures of the SVT and SSD, restrictions on the longitudinal vertex position can be relaxed, leading to a significant increase in the luminosity eventually used in many analyses. Integrated sampled luminosities for a Au+Au run of 8 weeks duration can be expected to be on the order of a few nb[-1], a substantial improvement over the expected 300 ub[-1] to be sampled in Run 7. This greatly benefits photon-hadron correlations for precision measurements of jet quenching and the reaction of the medium to energy deposited by the probe. The ultimate goal for such measurements at RHIC II requires an integrated luminosity of ~30 nb[-1] per year. The combination of the reduced material budget and the higher sampled luminosity will also benefit electron-hadron correlations, for both the separation of B and D contributions to non-photonic electrons and precise investigation of the energy loss of heavy quarks.
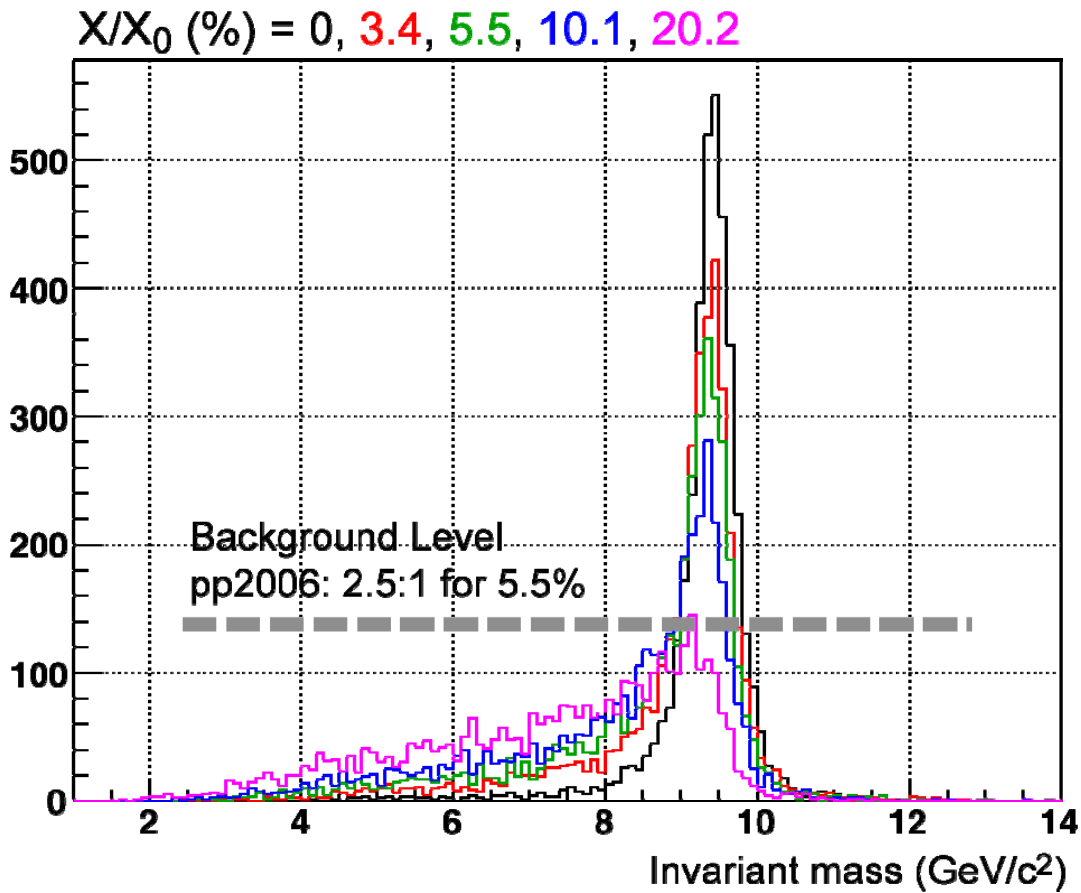

Figure 29: Upsilon 1S simulated line shape for different radiation lengths X/X_0 in the inner tracking system. Run 9 is expected to have $X/X_0 = 1.3\%$.

Bremsstrahlung of electrons impacts the precision of the Upsilon measurements, as illustrated in Fig. 29: the lower the material budget, the narrower is the line shape. A narrower line shape increases the statistical significance of the signal, and is also critical

for the challenging task of separating the 1S from the 2S and 3S states. Different Upsilon states are expected to be suppressed by different amounts in the medium, depending on the energy density. Sufficient integrated luminosity with low levels of material, combined with similar baseline measurements from Run 8, will lead to a major advance in the use of bottomonium to characterize the properties of the medium.

6. p+p beam Use request for Run 9

The STAR Collaboration proposes a polarized p+p run of (14+2) weeks in Run 9 to complete its 200 GeV program. The major goal for this run will be completing the two year goal of acquiring 80 pb^{-1} of total integrated luminosity necessary for a map of the x dependence of the spin-dependent gluon distribution of the proton, $\Delta G(x)$. CAD projections for beam delivery in Run 9 coupled with increased efficiency due to the DAQ1000 upgrade indicate this is an achievable goal (at mean performance) while allowing for moderate amounts of transverse running. STAR strongly prefers devoting pp collision time for data taking in Run 9 towards completion of its 200 GeV program (both longitudinal and transverse) for two reasons: (1) to attain adequate coincidence statistics for a given x-range ($\approx$ 0.04-0.08) at both 200 and 500 GeV which will provide a powerful crosscheck on the pQCD analysis of RHIC spin data and will constrain the evolution of the gluon helicity distribution; (2) the forward tracking upgrade needed to optimize STAR's performance for 500 GeV W production physics will not yet be installed in 2009.

7. Heavy Ion Beam use proposal for Run 10

The STAR Collaboration proposes a low $\sqrt{s_{NN}}$ Au+Au run of (12+3) weeks duration to make a definitive search for the existence and location of the QCD critical point.

The near-term upgrades planned by STAR should be complete by Run 10. Specifically, STAR expects to have completed the FMS, the DAQ1000 upgrade, and the TOF barrel detector upgrade. These upgrades will improve the performance of the STAR detector significantly (in some cases by an order of magnitude), and are crucial to fully optimize the search for the QCD critical point.

7.1 The search for the QCD critical point

There is a growing body of theoretical and experimental evidence that the critical point on the QCD phase diagram (Fig. 30), if it exists, should appear on the QGP transition boundary at baryo-chemical potential ~100 - 500 MeV, corresponding to heavy ion collisions with c.m. energy in the range 5 - 50 GeV/u.

Available results from LQCD [60] suggest that at non-vanishing chemical potential, as the temperature of dense hadronic matter increases it should undergo a rapid transition

from a hadron resonance gas to a quark-gluon plasma signaled by a sudden change in the equation of state. As the baryon chemical potential is increased, the fluctuations on the cross-over line increase dramatically suggesting the existence of a critical point in the phase diagram. As Fig. 31 shows, despite intense theoretical interest and effort using different LQCD approaches [61-63] which agree on the possible existence of a critical point, as yet there is no convergence on its possible location.

Verifying the existence of and locating this point with experimental measurements would be a major step forward in the world-wide effort to determine the properties of QCD at high temperature and density. Specifically, the discovery of the critical point would constitute the identification of a crucial landmark in the QCD phase diagram, key to understanding the phases of QCD and their quasi-particles.

In the vicinity of the critical point, critical fluctuations in parameters such as the baryon number density, quark number and charge occur. These should be reflected in the
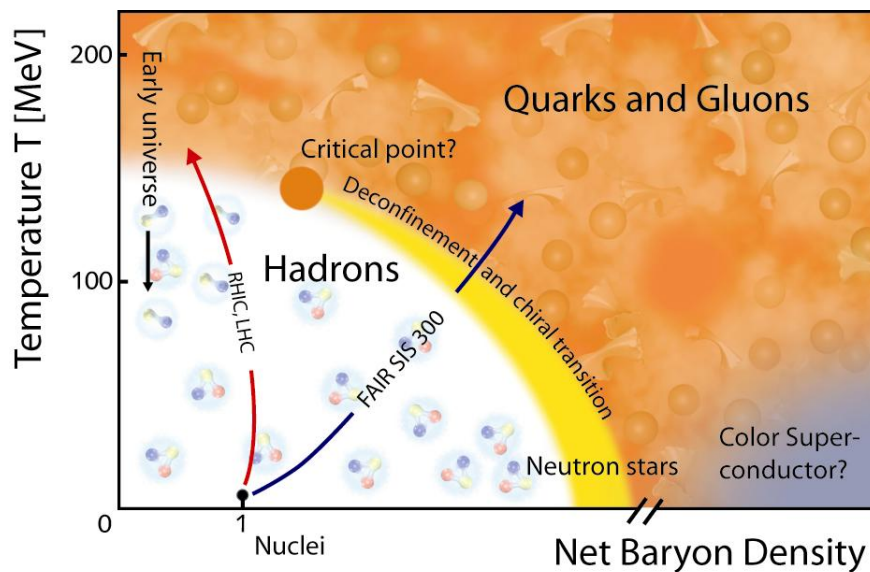

Figure 30. One of the major predictions of QCD in extreme conditions of high temperature or large baryon number density is the existence of a critical point at a particular temperature and density where a sharp distinction between the QGP phase and the hadronic phase first appears [64,65]. The QCD phase diagram, characterized by the temperature (T) and the baryon chemical potential μ_B, signifies the separation of QGP to hadronic phase. It is thought that for physical quark masses the first order phase transition line rises from the μ_B axis and terminates at the critical end point T_C, beyond which there is a rapid cross over in quantities such as the quark condensate [61,62,66,67]. Note that "focusing" in the μ, T plane by the hydrodynamic evolution of the system may cause many initial conditions to pass through the critical point region, broadening the signal region, and reducing the likelihood of sharp discontinuities.

laboratory in observables such as hadronic yields and particle ratios (T, μ_B), the collapse of proton elliptic flow, fluctuations in v_2, K/π, p/π, $<p_T>$ fluctuations and the scale dependence of the fluctuations which may reveal the source of the signal. The STAR detector, as a consequence of its large, uniform acceptance, and excellent PID capability with the inclusion of the TOF barrel upgrade has superb capability for carrying out the search for such effects and for providing definitive results on the existence and location of the QCD critical point.
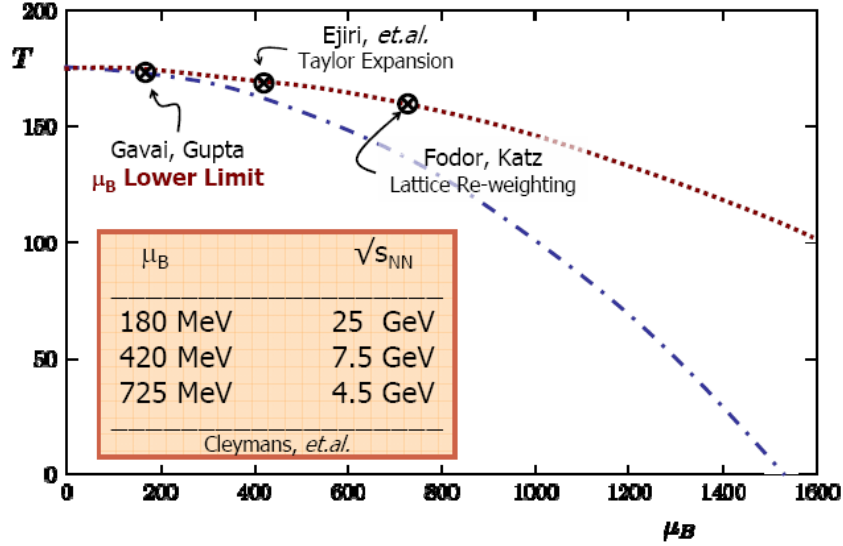

Figure 31. Comparison of three recent LQCD predictions on the possible location of the QCD critical point.

Simulations have shown that the change in the kinematic distribution of secondaries for low $\sqrt{s_{NN}}$ Au+Au running would not require specialized trigger counters. As shown in Table 2 for example, the simulations indicate that STAR's existing beam-beam counters will be adequate for triggering, and that centrality can be determined from a reference multiplicity. These simulations also demonstrate that the large 2π acceptance of STAR brings clear gains to this study as shown in the comparison of event plane resolution possible with STAR and NA49 (Fig. 32)

impact parameter	AuAu @ 5 GeV		AuAu @ 8.75 GeV	
	BBC Inner	BBC Outer	BBC Inner	BBC Outer
b<3	5	27	12	54
3<b<6	11	30	21	57
6<b<9	22	35	39	40

Table 2. Particle hit multiplicities in the STAR Beam-Beam counters for low $\sqrt{s_{NN}}$ Au+Au running

The desirability of full azimuthal acceptance is shown in Fig 33 where the apparent increase in the fluctuation measure $<\Delta p_{Ti} \Delta p_{Tj}>$ from failing to identify the underlying effects of a large scale correlation (in this case random orientation of the event plane for
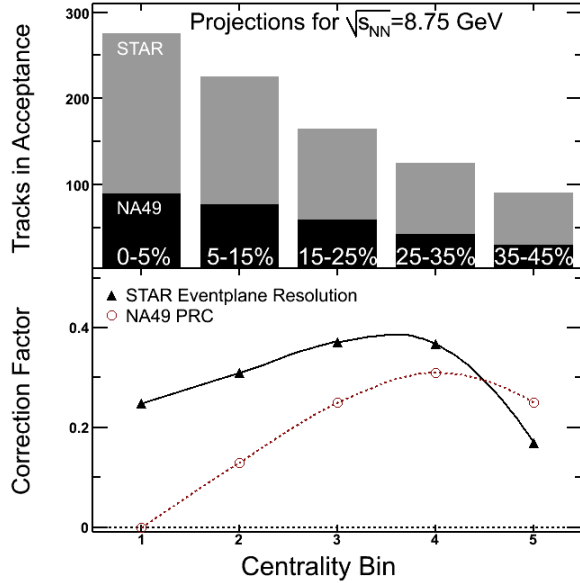

Figure 32. Simulation of the event plane resolution in STAR vs NA49 for comparable centrality bins ($\sqrt{s_{NN}} = 8.75$ GeV Au+Au (Pb+Pb)). From [68]
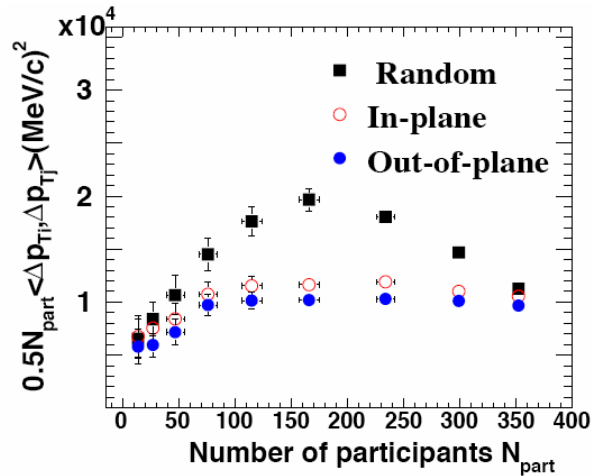

Figure 33. Contribution of elliptic flow to the apparent magnitude of $<\Delta p_{Ti} \Delta p_{Tj}>$ fluctuations for particles within 45 degrees of the event plane (red), 45 degrees of the out-of-plane direction (blue), and for a detector with partial angular coverage when the event plane is unknown (black). In the later case the fluctuations are overestimated because the event plane is fluctuating randomly in, out, and within the acceptance. From [68]

elliptic flow) is clearly evident. The conclusion is that a large 2π acceptance is essential for fluctuation measurements such as <p_T> fluctuations. The utility of such measures has already been demonstrated at high energy where the variance excess for <p_T> fluctuations has been inverted into p_T angular correlations which are then used to characterize elliptic flow and the near and away side medium response (Fig 34). These have proved an important tool for attempting to understand the role of elliptic flow, mini-jets, and medium response in producing the <pT> fluctuations forming an important baseline for the QCD critical point at lower energy as well.

As shown in Fig 35, it is also essential to have comprehensive particle identification capability within this acceptance to minimize the systematic error in searching for critical
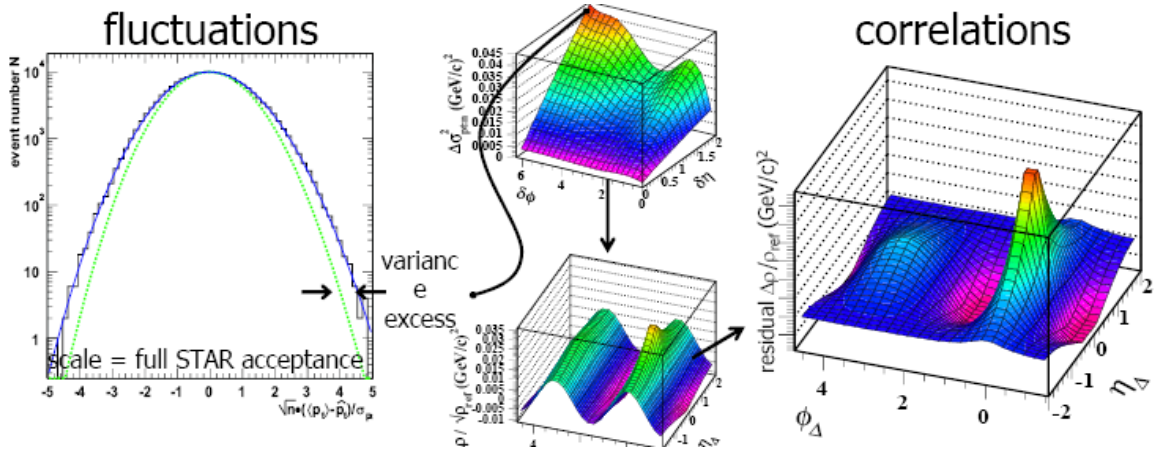

Figure 34. The variance excess from mean Pt fluctuations can be inverted to study the role of elliptic flow, mini-jets, and medium response to the correlations observed in Au+Au collisions.

fluctuations which might indicate the approach to the critical point. Systematic errors dominate the ultimate precision that is possible. As seen in the figure, based on simulation of 100,000 events at 40A GeV, the increase in statistical error without the full acceptance STAR TOF is from 5% to 11% (relative). However, a misidentification of only 1% leading to a swapping of pions for kaons reduces the width of the observed k/pi fluctuation distribution by 10%. A misidentification of 2% leads to a reduction in width of 20%. The conclusion from our simulations is that to optimize the potential to discover the QCD critical point a large 2π acceptance with excellent PID capability, which will be provided by the full acceptance TOF barrel, is essential.
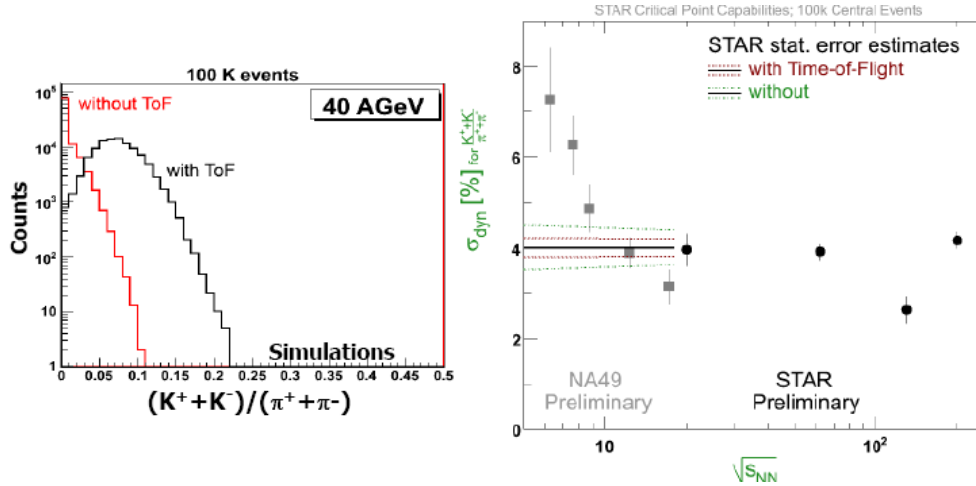
Figure 35. Study, based on 100,000 simulated events of the statistical and systematic uncertainties with and without the PID capability of the STAR TOF. From [68]

E c.m.	μ_B	BBC Coin Rate	#of days/1M (1day=10 hr)	#of events needed	#of days of beam
4.6	570	3	9	5M	45
6.3	470	7	4	5M	20
7.6	410	13	2	5M	10
8.8	380	20	1.5	5M	7.5
12	300	54	0.5	5M	2.5
18	220	>100	0.25	5M	1.5
28	150	>100	0.25	5M	1.5

Table 3: Strawman run plan for a QCD critical point search in Run 10
From [69]

For that reason, this study is performed most effectively once the STAR TOF Barrel upgrade is complete in Run 10. A strawman regarding the spacing of the energy points for such a scan, and the time necessary to acquire 5M events at each point is shown in Table 3. It suggests that a comprehensive search to determine the existence of a critical point in the QCD phase diagram can be completed by STAR in a data taking run of order 12 weeks long

8. Polarized proton request in Run 10

The STAR Collaboration further proposes a $\sqrt{s}$ = 500 GeV polarized p+p run of (8+3) weeks duration to begin its exploration of the flavor dependence of the sea quark/anti-quark polarization in the proton.

It is assumed that the expected performance of RHIC and STAR will complete the current $\sqrt{s}$ = 200 GeV spin program and that starting with run 10, STAR's priorities will switch to W production with $\sqrt{s}$ =500 GeV polarized pp collisions. The physics program at this energy will require very large integrated luminosity and running times to get statistics on parity violating W boson production to determine the polarization of anti-u and anti-d quarks. As this program is carried out, the spin-dependent gluon distribution of the proton, $\Delta G(x)$, will be measured as well. Again, di-jets and γ-jets will be the most effective at providing a map of $\Delta G(x)$ while inclusive jets and other channels will provide the first results. Eventually adequate statistics will allow a comparison of data at 200 and 500 GeV for an overlapping x-range ($\approx$ 0.04-0.08) but different Q^2 which will provide a powerful crosscheck on the pQCD analysis of RHIC spin data and will constrain the evolution of the gluon helicity distribution. STAR proposes to begin this multi-year program in run 10 with a request of 8+3 weeks of $\sqrt{s}$ =500 GeV polarized pp collisions.

9. Collaboration Readiness

The STAR Operations Group, as well as the STAR Collaboration membership plan an extensive program of shut-down activities in preparation for Run 8, including removal of of the present inner tracking system of STAR (SVT+SSD).

Steady progress is being made toward the construction of the TOF barrel upgrade that will be substantially implemented in time for a high statistics Au+Au run in FY09. According to the present project plan, 70% of the TOF barrel is expected to be ready for Run 9, with the full system complete and commissioned in time for Run 10. The DAQ1000 upgrade, which will increase STAR's data acquisition throughput by an order of magnitude will be operational by Run 9. A prototype of a new micro-vertex detector designed to operate in tandem with the existing Silicon Strip Detector (SSD) will begin construction during this period.

References

[1] J. Adams et al. (STAR Collaboration), Phys.Rev.Lett. **97**, 152302(2006).

[2] I. Arsene et al. (BRAHMS Collaboration), Phys. Rev. Lett. **93**, 242303 (2004).

[3] D. Kharzeev, Yu.V. Kovchegov, and K. Tuchin, Phys. Lett. B **599**, 23 (2004).

[4] A. Dumitru, A. Hayashigaki, and J. Jalilian-Marian, Nucl. Phys. A **765**, 464 (2006).

[5] D. Kharzeev, Nucl. Phys. A **715**, 35c (2003) ; D. Kharzeev, E. Levin, and L. McLerran, Nucl. Phys. A **748**, 627 (2005).

[6] S.S. Adler et al. (PHENIX Collaboration), Phys. Rev. Lett. **96**., 222301 (2006).

[7] V. Guzey, M. Strikman, and W. Vogelsang, Phys. Lett. B **603**, 173 (2004).

[8] L.C. Bland et al., Eur. Phys. J. C **43**, 427 (2005). See also [43].

[9] M. Diefenthaler [HERMES Collaboration], talk presented at 13th Intl. Workshop on Deep Inelastic Scattering, Madison, Wisconsin, April 2005 [hep-ex/0507013].

[10] W. Vogelsang and F. Yuan, Phys. Rev. **D 72**, 054028 (2005).

[11] J. Balewski, SPIN 2006 proceedings, hep-ex/0612036.

[12] A. Kocoloski, SPIN 2006 proceedings, hep-ex/0612005.

[13] L. Nogach, SPIN 2006 proceedings, hep-ex/0612030.

[14] D. Relyea, SPIN 2006 proceedings.

[15] F. Simon, SPIN 2006 proceedings, hep-ex/0612004.

[16] J. Webb, SPIN 2006 proceedings.

[17] Q. Xu, SPIN 2006 proceedings, hep-ex/0612035.

[18]A. Ogawa, SPIN 2006 proceedings.

[19] J. Adams *et al.* (STAR Collaboration), PRL **92**, 171801 (2004).

[20] D. Adams *et al*, (E704 Collaboration), PLB **261**, 201 (1991); \PLB 264, 462 (1991).

[21] J. Adams *et al.* (STAR Collaboration), PRL **97**, 152302 (2006).

[22] D. Sivers, PRD 41, 83 (1990); PRD **43**, 261 (1991).

[23] J.C. Collins, NPB **396**, 161 (1993).

[24] J. Qiu and G. Sterman, PRD **59**, 014004 (1998).

[25] A.V. Efremov, V.M. Korotiyan and O.V. Teryaev, PLB **348**, 577 (1995).

[26] C. Kouvaris *et al*., hep-ph/0609238.

[27] U. d'Alesio and F. Murgia, private communications.

[28] M. Diefenthaler {\it et al.} (HERMES Collaboration), Proceedings of the 13th International Workshop on Deep Inelastic Scattering (DIS2005), Madison, April 2005, hep-ex/0507013.

[29] D. Boer and W. Vogelsang, PRD **69**, 094025 (2004).

[30] W. Vogelsang, private communications

[31] C.J. Bomhof *et al*., hep-ph 0701277.

[32] K.H. Ackermann *et al.* (STAR Collaboration), NIMA **499**, 624 (2003).

[33] B.Jaeger, M. Stratmann and W. Vogelsang, PRD **70**, 034010 (2004).

[34] M. Stratmann and W. Vogelsang, PRD **70**, 034010 (2004).

[35] B.I. Abelev *et al.* (STAR Collaboration), PRL **97**, 252001 (2006).

[36] F. Simon *et al.* (STAR Collaboration), Proceedings of the
Conference on the Intersection of Particle and Nuclear Physics (CIPANP 2006), Puerto Rico, June 2006.

[37] B.A. Kniehl, G. Kramer and B. Poetter, NPB **597**, 337 (2001).

[38] Q.H. Xu, Z.T. Liang and E. Sichtermann, PRD **73**, 077503 (2006).

[39] D. de Florian, M. Stratmann and W. Vogelsang, PRD **81**, 530 (1998).

[40] M. Stratmann, Proceedings of the 14th International Workshop on Deep Inelastic Scattering (DIS2006), Tsukuba, April 2006.

[41] Alessandro Bacchetta et al. *The Sivers single-spin asymmetry in photon-jet production*, hep-ph 0703153.

[42] G. Bunce *et al*., Ann. Rev. Nucl. Part. Sci. **50** (2000) 525; C. Aidala, *et al.* Formal Report BNL-73798-2005 (2005).

[43] S. Bültmann et al., Phys. Lett.**B579** (2004) 245.

[44] S. Bültmann et al., Nucl. Instr. Meth. **A535** (2004) 415.

[45] W. Guryn et al., RHIC Proposal R7 (1994) (unpublished).

[46] V. Barone, E. Predazzi, *High-Energy Particle Diffraction*, Texts and Monographs in Physics, Springer-Verlag (2002) ISBN: 3540421076.

[47] S. Donnachie, G. Dosch, P. Landshoff, *Pomeron Physics and QCD*, Cambridge University Press (1998) ISBN: B0006Z3XLM.

[48] A. Bravar, W. Guryn, S.R. Klein, D. Milstead, B. Surrow, J.Phys. G28 (2002) 2885.

[49] E. Leader, *Spin in Particle Physics*, Cambridge University Press (2001), ISBN: 0521020778.

[50] N. H. Buttimore, B. Z. Kopeliovich, E. Leader, J. Soffer, T. L. Trueman, Phys. Rev. **D59**, (1999) 114010.

[51] N.H. Buttimore, E. Leader, T.L. Trueman, Phys. Rev. **D64** (2001) 094021.

[52] E. Leader and T. L.Trueman, Phys. Rev. **D61**, (2000) 077504.

[53] F. Close, Reports on Progress in Physics **51** (1988) 833 and F. Close, A. Kirk and G. Schuler, Phys. Lett. **B477** (2000) 13.

[54] D. Barberis et al., WA102 Collaboration, Phys. Lett. **B479** (2000) 59.

[55] L. Ruan et al. (STAR Collaboration), "Physics with identified particles in STAR", nucl-ex/0701070, from QM2006.

[56] M. Calderon et al. (STAR Collaboration),"STAR results on high transverse momentum, heavy flavor, and electromagnetic probes", nucl-ex/0701070, from QM2006.

[57] W. Dong PhD thesis, "Measurement of non-photonic electron azimuthal anisotropy v_2 from Au+Au collisions at sqrt(s_{NN}) = 200 GeV", UCLA 2006.

[58] J. Adams et al (STAR Collaboration), Phys. Rev. Lett. **94** 062301 (2005).

[59] G. David, R. Rapp, Z. Xu, "Electromagnetic Probes at RHIC-II", nucl-ex/0611009.

[60] See for example, F. Karsch, "Lattic Results on the QCD Critical Point", RIKEN-BNL Workshop, "Can we discover the QCD Critical Point at RHIC", March 9-10, 2006, Brookhaven National Laboratory: https://www.bnl.gov/riken/QCDRhic/talks.asp

[61] Z. Fodor, S.D. Katz, JHEP 0203:014,2002, hep-lat/0106002

[62] R.V. Gavai, Sourendu Gupta, Phys.Rev.D71:114014,2005, hep-lat/0412035

[63] F. Karsch, hep-lat/0601013

[64] F. Wilczek, hep-ph/0003183

[65] F. Wilczek, Nucl.Phys.A663:3-20,2000, hep-ph/9907340

[66] M.A. Stephanov, K. Rajagopal, E.V. Shuryak, Phys.Rev.Lett.81:4816-4819,1998, hep-ph/9806219

[67] M.A. Stephanov, K. Rajagopal, E.V. Shuryak, Phys.Rev.D60:114028,1999, hep-ph/9903292

[68] P. Sorensen, *STAR Plans for Low Energy Running,* Workshop on Future Prosepcts in QCD at High Energy: A joint EIC2006 and Hot QCD Meeting, July 17-22, 2006, Broohaven National Laboratory: http://rhic.physics.wayne.edu/~bellwied/qcdfp/qcdfp-sorensen.ppt

[69] T. Nayak, "Experiments with STAR near the Critical Point", RIKEN-BNL Workshop, "Can we discover the QCD Critical Point at RHIC", March 9-10, 2006, Brookhaven National Laboratory: https://www.bnl.gov/riken/QCDRhic/talks.asp